

79-11-352  
高工研圖書室

# DEUTSCHES ELEKTRONEN-SYNCHROTRON **DESY**

DESY 79/68  
October 1979

## HIGH ENERGY BEHAVIOR OF NONABELIAN GAUGE THEORIES

by

J. Bartels

*II. Institut für Theoretische Physik der Universität Hamburg*

NOTKESTRASSE 85 2 HAMBURG 52

To be sure that your preprints are promptly included in the  
HIGH ENERGY PHYSICS INDEX ,  
send them to the following address ( if possible by air mail ) :

DESY  
Bibliothek  
Notkestrasse 85  
2 Hamburg 52  
Germany

DESY 79/68  
October 1979

1

Abstract:

The high energy behavior (in the Regge limit) of nonabelian gauge theories is reviewed. After a general remark concerning the question to what extent the Regge limit can be approached within perturbation theory, we first review the reggeization of elementary particles within nonabelian gauge theories. Then the derivation of a unitary high energy description of a massive (= spontaneously broken) nonabelian gauge model is described, which results in a complete reggeon calculus. There is strong evidence that the zero mass limit of this reggeon calculus exists, thus giving rise to the hope that the Regge behavior in pure Yang-Mills theories (QCD) can be reached in this way. In the final part of these lectures two possible strategies for solving this reggeon calculus (both for the massive and the massless case) are outlined. One of them leads to a geometrical picture in which the distribution of the wee partons obeys a diffusion law. The other one makes contact with reggeon field theory and predicts that QCD in the high energy limit is described by critical reggeon field theory.

High Energy Behavior of Nonabelian Gauge Theories +)

J. Bartels

II. Institut für Theoretische Physik, Universität Hamburg

+)

Lectures given at

XIX Cracow School of Theoretical Physics, Zakopane, June 1979

and

X GIFT Seminar on Theoretical Physics, Jaca, June 1979

and

IX International Summer Institute on Theoretical Physics, Kaiserslautern,

August 1979

## I. Introduction

These lectures intend to give a review of our present understanding of the Regge limit of nonabelian gauge theories, in particular QCD. Since cross sections are large in this kinematic regime, high energy physicists have always been interested in understanding the dynamics behind it (especially the nature of the Pomeron), but a theoretical description which is based on an underlying quantum field theory is still missing. Most previous attempts to understand the Regge limit within a field theory have been based on perturbation theory, and the main difficulty (besides the question which field theory to choose) was that the number of Feynman diagrams that could be handled always turned out to be too small. Now QCD is believed to be the right theory of strong interactions, and we are asked to understand its behavior in the Regge limit. Can we hope that the conventional approach, i.e. the start from perturbation theory, might be successful for this theory? Let me say a few words about this general question, before I come to details. The point I would like to make is that there are good reasons to believe that perturbation theory is a useful starting point, because the Regge limit is not far from that kinematic region in which perturbation theory works (hard scattering processes). But, on the other hand, the Regge limit is also sensitive to certain features which are commonly referred to as nonperturbative.

Let us start with the optimistic part of the argument and consider elastic forward scattering of a very heavy photon off a nucleon. This is the process measured in deep inelastic leptonproduction (Fig.1), and the standard argument about light cone dominance tells us that in the Bjorken limit ( $-q^2 \rightarrow \infty$ ,  $s \sim -q^2 (\frac{1}{x} - 1) \rightarrow \infty$ ,  $x$  fixed) one probes the short distance structure of the nucleon target: if  $\gamma_1$  and  $\gamma_2$  are the two space-time points where incoming and outgoing photons couple to the nucleon, then  $(\gamma_1 - \gamma_2)^2 \sim -1/q^2$ . Within QCD the property of asymptotic freedom then allows to use perturbation theory for this short distance process. Either by means of the operator expansion and renormalization group techniques or, equivalently, by extracting and summing leading logarithms of Feynman diagrams, one can calculate the  $q^2$ -dependence, i.e. the change of the cross section when we move closer and closer to the light-cone ( $\gamma_1 - \gamma_2$ )<sup>2</sup> = 0. We now imagine that at some large value of  $q^2$  we take a different limit: keeping now  $q^2$  fixed and taking  $x \rightarrow 0$ , we reach the Regge limit  $\cos \Theta_t \sim s/\sqrt{-q^2} \rightarrow \infty$ . By choosing  $q^2$  large enough, our investigation of the Regge limit can be carried out very close to the light cone, but once  $q^2$  is kept fixed we always

stay away from it by some finite distance. In terms of QCD Feynmann diagrams it is not difficult to see that those diagrams (Fig.1) which govern the leading  $q^2$ -behavior of the Bjorken limit cannot be expected to correctly also describe the region of very small  $x$ . The tower diagrams of Fig.1 do not contain "final state interactions" of the produced quarks and gluons and, hence, cannot satisfy unitarity which is known to be important in the Regge limit ( $x \rightarrow 0$  limit). If one wants to investigate the Regge limit within this perturbative approach, it is, therefore, necessary first to find all Feynmann diagrams (beyond those of Fig.1), which are required by unitarity for yielding a sensible  $x \rightarrow 0$  behavior, then to compute their behavior in the limit  $x \rightarrow 0$ .

We conclude from this that, since the Regge limit, i.e. the Pomeron, can be investigated very close to the light cone where the (effective) coupling constant is small and perturbation theory works, perturbation theory may be a good starting point also for studying the Pomeron. The problem then consists of two major parts: first one has to decide which terms in the perturbation expansion (Feynmann diagrams) have to be taken into account. Because of unitarity which is crucial for the Pomeron physics, these terms will not be the same as those which govern the Bjorken limit. Secondly, one has to find a method for summing them up. As I will make clear later, this part of the problem will require new techniques.

But as I have already indicated before, the Pomeron is also sensitive to certain features of long distance physics ("confinement dynamics"), which implies that at some stage nonperturbative aspects might have to enter the calculations. In the elastic scattering process of a very energetic hadron (say, in the rest frame of the target) the projectile appears as a composite system of partons which are spread out in impact parameter space. The probability of finding a slow parton at distance  $b$  is given by the impact parameter transform of the elastic scattering amplitude:

$$\frac{1}{s} T(s, b^2) = \frac{1}{2\pi s} \int d^2 k_{\perp} e^{-i k_{\perp} b} T(s, k_{\perp}^2 = -t). \quad (1.1)$$

The hadron radius is defined as:

$$\langle b^2 \rangle = \frac{1}{s} \int d^2 b \ b^2 T(s, b^2) \quad (1.2)$$

and, in general, it will depend on the energy  $s$ . It might, again, be useful to relate this to the hard scattering process in the Bjorken limit. In the deep inelastic scattering process the photon couples just to those constituents of the hadron which carry the fraction  $x$  of the hadron momentum ( $x$  is the Bjorken scaling variable). When approaching the Regge limit  $x \rightarrow 0$ , these constituents are more and more wee: the Pomeron feels the distribution of the wee partons inside the hadron. When the energy increases, i.e. the incoming hadron becomes more energetic, more decay processes are necessary before a fast parton slows down and eventually creates wee partons, and this may occupy a larger region in impact parameter space. As a result, the radius  $\langle b^2 \rangle$  may grow as a function of  $s$ . In order to estimate how fast this growth could be in a realistic model, it may be useful to recall the multiperipheral model where

$$\frac{1}{s} T(s, b^2) = \frac{\text{const} \cdot e^{-b^2/4\alpha' \ell n s}}{\alpha' \ell n s} \quad (1.3)$$

and

$$\langle b^2 \rangle = \text{const} \cdot \alpha' \ell n s \quad (1.4)$$

( $\alpha'$  is the Pomeron slope). Lowest order perturbation theory (Fig.2) in a field theory with massless vector particles <sup>2)</sup>, on the other hand, leads to

$$\frac{1}{s} T(s, b^2) \sim |b|^{-4} \quad (1.5)$$

$$\langle b^2 \rangle = \infty \quad (1.6)$$

This indicates that only after summing many more diagrams one may hope to come somewhat close to (1.3), (1.4): the quantity  $\langle b^2 \rangle$  can serve as a guide in estimating to what extent the use of perturbation theory alone is sufficient to "confine" the wee partons inside the fast hadron, and the fact that it is infinite in lowest order perturbation theory of QCD indicates how difficult it may be to obtain a correct theory of the Pomeron.

Before I can start to describe how well understood the Pomeron is within

nonabelian gauge theories (and this understanding is almost entirely based on perturbation theory), I have to mention the other approach towards a theory of the Pomeron, namely reggeon field theory (RFT). As it is well known <sup>3)</sup>, physics of the Pomeron is most easily be discussed in terms of singularities in the angular momentum plane, and the interaction of moving pole and cut singularities has been formulated by Gribov in his reggeon calculus (or reggeon field theory). The rules of this formalism follow from certain analyticity properties of the S-matrix (existence of partial wave continuation, and t-channel unitarity equations) and are expected to hold in field theories that contain moving Regge singularities. The values of the parameters of reggeon field theory (intercepts, slopes, and interaction vertices), however, are not very much constrained from these analyticity arguments alone, and as long as RFT has not been considered in the context of a specific underlying field theory, they have been chosen freely. As the most interesting case, the Pomeron with intercept one has been studied extensively, and the best-known result is the critical Pomeron theory with

$$\sigma_{\text{total}} \sim (\ell n s)^{-1} \quad , \quad \rho \sim 0.2 \quad (1.7)$$

Since this solution has also been shown to be consistent with the most restrictive constraints imposed by s-channel unitarity, it is an excellent candidate for a theory of strong interactions at high energies. More recently <sup>4)</sup>, also the case of the Pomeron intercept being above one has been investigated. Apart from the question how presently available energy ranges fit into these Pomeron field theories, the outstanding theoretical problem remains the derivation of the Pomeron parameters from an underlying field theory, such as QCD. It is not unexpected that these features of angular momentum theory will play an important role in analyzing the high energy behavior of nonabelian gauge theories.

After this introduction I can begin with a brief outline of the program of my talk. The aim is a review of what at present we know about the Regge limit (i.e. the Pomeron) of nonabelian gauge theories, and since the problem has not yet been solved completely, I shall attempt to describe both what has been achieved so far and what seem to be the main strategies for the future. Most of the existing calculations are determined to find the high energy behavior of QCD, the theory of (confined) quarks and gluons, but mainly because of the infrared problems, they

start from spontaneously broken gauge theories. The mass of the vector particles then is considered to be an infrared cutoff which at the end of the calculations is taken to zero, hoping that in this limit one reaches QCD. As I have said already, all this will be based on perturbation theory.

In the first two sections of my talk I shall outline our present understanding of what the formal behavior of massive (=spontaneously broken) nonabelian gauge theories is in the Regge limit. First I shall discuss the question of reggeization of elementary particles in these theories which divides the gauge theories into two classes: those where (at least) all vector particles reggeize and those where some of them don't. Then I shall describe (for a simple model) how this property of reggeization is seen to lead to a full reggeon calculus: this follows from the requirement of having (asymptotic) unitarity in both  $s$  and  $t$  channel, and the elements of the reggeon calculus are calculable in the limit of small coupling constant. Although such a reggeon calculus is of interest by itself, I shall consider it mainly as an intermediate step on the way towards finding the high energy behavior of massless Yang-Mills theories. This then requires a study of the zero mass limit of the reggeon calculus, and I shall briefly discuss what we know about this limit. As to the question how the use of perturbation theory may be extended into the Regge limit, this first part of my talk then basically selects all those terms in the perturbation expansion which have to be taken into account for a reliable high energy description: the selection criterion is unitarity, and the Feynmann diagrams which are included in the reggeon calculus are just enough to satisfy unitarity.

Section IV deals with the question of how to solve this reggeon calculus, i.e. how to perform the summation of all the terms that we have decided to keep. First I shall briefly sketch an approach which, although it has not been pushed very far yet, has the advantage of asking directly for the distribution of the wee partons in impact parameter space. It allows a rather direct control over  $\langle b^2 \rangle$  and, according to what has been said in the introduction, over the validity of the use of perturbation theory. Moreover, this technique seems to be applicable also to QED, where a high energy description which takes full account of unitarity is still missing. Within this approach one sees the possibility that, after summing all terms that have been obtained in the first part, the distribution of wee partons may come close to the multiperipheral picture. Then I shall describe how one might use the full apparatus of reggeon field theory, in particular its phase structure

as a function of the bare Pomeron intercept, in order to determine the high energy behavior of massless Yang-Mills theories. Under the assumption that confining QCD can be obtained as the zero mass limit of spontaneously broken gauge theories with a modified  $i\epsilon$ -prescription, this approach predicts critical high energy behavior for QCD, i.e.  $\sigma_{total} \sim (Lns)^{\frac{1}{2}}$ .

## II. Reggeization in Yang-Mills theories

Let us first consider gauge theories quite in general and ask which of them can be expected to have a "good" high energy behavior. The requirements one would like to impose on a realistic theory are the existence of moving Regge singularities and analyticity of the scattering amplitudes in the complex angular momentum plane. In particular, one would not like to have fixed singularities of the Kronecker delta function type which seem to exist if the theory contains nonreggeizing particles. This leads us to the question of reggeization in Yang-Mills theories.

It might be useful to recall what reggeization of a particle in a given field theory means. Suppose the theory contains a particle with spin  $J_0$  and mass  $\mu$ . The exchange of this particle in lowest order perturbation theory (Fig.3) yields the following contribution to the t-channel partial wave:

$$T(J, t) = \text{const} \cdot \int_{J_0}^J J' \quad (2.1)$$

which is nonanalytic in  $J$ . Higher order diagrams for the same amplitude then can have two possible effects: either they leave the lowest order term (2.1) unchanged and simply add some new contributions:

$$T(J, t) = \text{const} \cdot \int_{J_0}^J J' + \text{terms analytic near } J_0. \quad (2.2)$$

In this case the particle stays elementary and leads to a nonanalytic term in the partial wave amplitude. Alternatively, the higher order contributions remove the  $\delta$ -function in (2.1), for example:

$$T(J, t) = \frac{\alpha(t) - J_0}{\alpha(t) - J} \cdot \text{const} \quad (2.3)$$

$$\alpha(t) = J_0 + (t - \mu^2) \cdot \beta(t) \quad (2.4)$$

( $\beta(t)$  is proportional to the coupling constant of the theory and vanishes in lowest order perturbation theory. Eq.(2.3) then reduces to (2.1)). In this case the particle is said to reggeize: it lies on the trajectory (2.4), and the partial wave (2.3) is analytic in  $J$ . Experience with strong interaction physics clearly favors this second alternative: there is no evidence that singularities of the type (2.1) should be present. Therefore, one should look for theories in which, if possible, all particles reggeize.

Is there a simple way to decide whether, in a given theory, a particle reggeizes or not? The safest way, of course, is the explicit calculation: one computes the next-to-lowest order term of the partial wave and com-

pare with the power series expansion of (2.3). This is the method by which, in the early sixties, Gell-Mann et.al.<sup>5)</sup> found that the fermion in massive QED lies on a Regge trajectory. Based on these calculations the same authors derived certain criteria which must be satisfied if a particle is to reggeize. One of them implies that the theory must contain particles of spin one (or higher spin). This excludes scalar theories such as  $\varphi^3$  or  $\varphi^4$  (although these theories may still contain moving Regge singularities). Another criterion requires certain factorization properties of the Born amplitudes. Later on, Mandelstam<sup>6)</sup> gave counting arguments which say under what conditions a particle must necessarily reggeize. All those methods, when applied to (massive) QED, agree in that the fermion reggeizes but the photon does not. The boson in scalar QED has also been found<sup>7)</sup> to reggeize: this result came out only after direct calculation of Feynmann diagrams up to eighth order, and it illustrates that factorization and counting arguments<sup>8)</sup> have to be applied with great care.

Theories in which also the vector particle reggeizes must be of the non-abelian type. To be more specific let us consider models of the following kind:

$$\mathcal{L} = -\frac{1}{4} F_{\mu\nu}^a F^{\mu\nu a} + \frac{1}{2} (\partial_\mu \phi)^2 - V(\phi) + \text{spinor part} \quad (2.5)$$

$$F_{\mu\nu}^a = \partial_\mu A_\nu^a - \partial_\nu A_\mu^a + g f^{abc} A_\mu^b A_\nu^c \quad (2.6)$$

$$\partial_\mu \phi = (\partial_\mu - ig A_\mu^a T^a) \phi \quad (2.7)$$

$$[T^a, T^b] = i f^{abc} T^c. \quad (2.8)$$

The potential  $V(\phi)$  is invariant under the gauge group  $G$  and has its minimum at some nonzero value  $\langle \phi \rangle \neq 0$ . The pattern of spontaneous symmetry breaking may be rather complicated (for general symmetry breaking schemes see, for example, Refs.9 and 10), and the resulting particle spectrum may mask the original gauge group  $G$ . Is there a simple criterion which tells us under which conditions the vector particles reggeize? We first answer the question for two popular models: (i) the

Higgs SU(2) model and (ii) the Weinberg-Salam model, and then state the result for the general case.

For the first case the gauge group G is SU(2), and the scalar field comes in two SU(2) doublets. With the scalar potential

$$V(\phi) = -\frac{1}{2}\mu^2\phi^2 + \frac{\lambda}{4}(\phi^2)^2 \quad (2.9)$$

the Higgs mechanism makes all three vector particles massive:

$$M^2 = g^2\mu^2/\lambda, \quad (2.10)$$

and leaves one (massive) scalar particle. (Generalization to SU(n) is made in the following way <sup>11</sup>): one starts from the gauge group U(n), adds n complex fundamental representations of scalar fields which make all n<sup>2</sup> vector particles massive, and then restricts oneself to the SU(n) subgroup of U(n). Using the factorization criterion of the Born amplitudes, Grisaru et al. <sup>11</sup> found that both the fermions and the vector particles of this model reggeize. For the scalar the situation is still somewhat unclear: recently <sup>8</sup> it has been pointed out that it may reggeize, but in a more complicated way, similarly to the boson in scalar QED. This is contrary to the former belief <sup>12</sup> that reggeization of the scalar particle can occur only for special values of the parameters of the theory (masses and coupling constants). Presumably, only calculations similar to those of Ref. 7 will settle this point.

For the Weinberg-Salam model with gauge group G = SU(2) x U(1) one adds one doublet of complex scalar fields:

$$\mathcal{L} = -\frac{1}{4}F_{\mu\nu}^2 + \frac{1}{2}\partial_\mu\phi^T\partial_\nu\phi + \frac{1}{2}(\partial_\mu\phi)^\dagger(\partial_\nu\phi) + V(\phi) + \mathcal{L}(\text{spinors}) \quad (2.11)$$

$$\mathcal{B}_{\mu\nu} = \partial_\mu\partial_\nu - \partial_\nu\partial_\mu \quad (2.12)$$

$$V(\phi) = -\mu^2\phi^T\phi + \lambda(\phi\phi^\dagger)^2 \quad (2.13)$$

As a result of the Higgs mechanism one has the three massive vector bosons:

$$W_\mu^\pm = \frac{1}{\sqrt{2}}(A_\mu^1 \mp iA_\mu^2) \quad (2.14)$$

$$Z_\mu = \frac{-gA_\mu^3 + g' B_\mu}{\sqrt{g^2 + g'^2}} \quad (2.15)$$

$$g' = g \cdot \tan\theta_W \quad (2.16)$$

and the massless photon:

$$A_\mu = \frac{gB_\mu + g'A_\mu^3}{\sqrt{g^2 + g'^2}} \quad (2.17)$$

With the same arguments which have been used for the Higgs model one finds <sup>13</sup> that in the Weinberg-Salam model only the W-bosons reggeize whereas the Z and the photon don't. Obviously, it is the U(1) subgroup of G which destroys the reggeization: the W's being purely made out of the nonabelian A-fields still reggeize. The Z and the photon, on the other hand, contain the U(1)-type B-field, which destroys the reggeization.

The general connection between the structure of the gauge group G and the reggeization of the vector particles has recently been investigated by two groups <sup>13</sup> 14). It turns out that in order to make all vector particles reggeize G must be simple or semisimple. If G does not have this property - in particular if it has an abelian invariant subgroup - some of the gauge particles lie on Regge trajectories, but others do not reggeize. The Higgs model with G = SU(2) and the Weinberg-Salam model with G = SU(2) x U(1) are examples for these two types of models. It is important to note that this result on the reggeization depends on the gauge group G but not on the way in which the Higgs scalars enter: this may introduce additional (global) symmetries into the theory, which manifest themselves in the mass spectrum of the vector particles but are independent of G. Finally, if after invoking the Higgs mechanism some vector particles are left massless, their trajectory functions (if they reggeize) have to be regularized by some infrared cutoff (cf.



(2.4)).

The most important implication of this result concerns the reggeization of the photon within grand unification schemes. In one of the most popular versions<sup>15)</sup>, weak, electromagnetic, and strong interactions are embedded into a SU(5) gauge theory in which, according to the result stated above, all vector particles reggeize:

$$SU(2) \times U(1) \times SU(3)_{color} \subset SU(5). \quad (2.18)$$

Such a scheme, for the first time, would allow to get rid of the undesired Kronecker-type partial wave singularities connected with the abelian photon, which according to our present understanding of this problem persist in QED and also the Weinberg-Salam model.

III. Construction of a (asymptotically) unitary S-matrix in a massive Yang-Mills theory. The zero-mass limit.

In this section I come to the longest part of my talk. Concentrating on the SU(2) - Higg's model which has been introduced in the previous section, I would like to describe how one can construct a high energy description of this model which satisfies (in an asymptotic sense) unitarity in both the direct and the crossed channel. The mass of the vector particle mainly serves as a convenient way to avoid the problems connected with massless particles and will be kept different from zero until the end of this section where I will mention what is known about the zero mass limit. The logic of this approach for investigating the high-energy behavior of massless Yang-Mills theories is illustrated in Fig.4a and b: in the massive case one studies the high energy behavior of processes with the (massive) vector bosons as external particles. In order to be able to take the zero mass limit, one has to replace the external particles by appropriate hadron wave function models. The gluon "soup" exchanged between these hadrons (the box of Fig.4b) is taken to be the zero mass limit of the box of Fig.4a. Within the line of arguments set up in the introduction the requirement of having for the massive case unitarity serves as a guide in selecting those terms in perturbation theory which one has to sum up for having a reliable description of the Regge limit of massless gauge theories.

After having established that the massive vector particles of the Higgs model reggeize, it seems very natural to expect that the full high energy description of this field theory should come in form of a complete reggeon calculus: the three reggeons (i.e. the reggeized vector particles) interact with each other through all possible (momentum dependent) interaction vertices which are allowed by signature conservation. This will, in fact, be the result of this section: starting from the requirement of both s and t-channel unitarity, a full reggeon calculus emerges. The method I am going to describe also allows, at least in principle, to compute the elements of this reggeon calculus.

Before I am going into more detail, a few words should be said about the method of calculation. So far the problem of finding a reliable description for the high energy behavior of a field theory has not been solved, and this failure has, at least in part, to do with the calculational technique. For each order of perturbation theory the high energy behavior of a scattering amplitude, say for the  $2 \rightarrow 2$  process, can be written as:

$$g^{2n} s [ (\ell ns)^{n-1} f_{n-1}(t) + (\ell ns)^{n-2} f_{n-2}(t) + \dots + (\ell ns) f_1(t) + f_0(t) ] + O(s^0) + O(s^{-1}) + \dots \quad (3.1)$$

Conventionally, the leading term of this expansion,  $f_{n-1}(t)$ , is found by writing down all Feynmann diagrams of this order perturbation theory, and, by means of a clever parametrization (Sudakov variables, infinite momentum variables,  $\alpha$ -parameter representation), extracting the highest power of  $lns$ . Summation over all orders in  $g$  then yields the leading -logarithmic approximation (LLA). As it turns out, however, in both QED and nonabelian vector theories this approximation violates the Froissart bound and, hence, is unacceptable. Because of the tremendous technical complications, the nonleading terms in (3.1)  $f_{n-2}, \dots, f_0$  can be computed so far only for very few special cases (for recent progress in this direction see Ref.16), but not for the vector theories we are interested in. In order to make further progress it seems, therefore, necessary to look for other methods of computation.

Since the main defect of the LLA was the violation of the Froissart bound, i.e. the lack of unitarity, the first goal must be restoration of unitarity. This suggests to use unitarity for the construction of the amplitudes from the very beginning: the Lagrangian is used only for determining vertices in the tree approximation. Amplitudes and all higher order corrections are then found by means of dispersion relations, i.e. by using our knowledge about the analytic structure of multiparticle amplitudes in the Regge limit. This guarantees s-channel unitarity and, thanks to the reggeization of the vector particle, also t-channel unitarity in terms of partial wave unitarity. In terms of the expansion (3.1), presumably only parts of the nonleading coefficient functions  $f_{n-2}, \dots$  can be found in this manner: those which are necessary for achieving unitarity. In other words, what one obtains is likely to be the small-g approximation of the unitary S-matrix (which does not agree with the LLA). Whether this approximation is sufficient to give a reliable high energy theory can, at earliest, be answered after the summation of all these terms has been carried out. This problem will be subject of the next part of my lectures.

The presentation of how the construction of the unitary S-matrix works

will be organized in the following way. Since extensive use will be made of the analytic structure of multiparticle amplitudes in the Regge limit, I start (part A) with a short review of those features which will be needed in the following. Then (part B) the construction of  $T_{n \rightarrow m}$  in the LLA will be described. In part C this approximation will be unitarized, leading to the full reggeon calculus. In the final part D I shall discuss features of the zero mass limit.

A. Analytic structure of multiparticle amplitudes at high energies.

Throughout this section I shall take a very pragmatic attitude: rather than describing any proofs or derivations, I shall restrict myself to listing those results which will be needed in the following. Those who wish to learn more details I refer to the lectures of Stapp and White (17) in the Les Houches Summer School 1975 and to Refs. 18-20.

Let me first recall a few well known facts about the  $2 \rightarrow 2$  amplitude at high energies:

- (i)  $T_{2 \rightarrow 2}$  satisfies a dispersion relation in  $s$  with right and left hand cuts. For a theory with vector particles one needs two subtractions.
- (ii) Real and imaginary part of the amplitude are connected via the signature factor:

$$T_{2 \rightarrow 2} = \frac{1}{2\pi i} \int ds \left( -i + \frac{\cos \pi j + \tau}{\sin \pi j} \right) F(j, t) \quad (3.2)$$

The partial wave  $F(j, t)$  is real in the physical region of the s-channel.

(iii) t-channel unitarity comes in form of partial wave unitarity relations. Starting from the normal t-channel unitarity equations, for example:

$$disc_t T = \text{Diagram} + \dots \quad t \gg (s_\mu)^2 \quad (3.3)$$



one projects out the partial waves  $F(j, t)$ , assumes that the two pairs of intermediate state particles couple together to moving Regge poles and continues down to  $t < 0$ :

This decomposition is necessary for both s and t-channel unitarity. In the s-channel the Steinmann relations forbid simultaneous discontinuities in energy variables of overlapping channels (in the present case, the (ab) and (bc) channels are mutually overlapping). This problem is avoided when  $T_{2 \rightarrow 3}$  is written as in (3.7). Modern dispersion theory also proves that both pieces in (3.7) (or Fig.6) have only normal threshold singularities in their respective energy variables: more complicated singularities, such as Landau singularities, are subdominant in the double Regge limit. From the t-channel point of view the decomposition (3.7) is important, because only in this representation the partial waves  $F_L$  and  $F_R$  are real, i.e. free from internal phase factors. For both  $F_L$  and  $F_R$  a reggeon calculus exists <sup>20)</sup> which satisfies t-channel partial wave unitarity.

We are now in the position to list the properties analogous to (i)-(iii). Once the decomposition (3.7) (or Fig.6) of  $T_{2 \rightarrow 3}$  has been made, we have:

- (i) each of the two terms satisfies a double dispersion relation (with both right and left hand cuts and the appropriate number of subtractions).
- (ii) Real and imaginary parts are related through the signature factors (3.8).
- (iii) For each partial wave a reggeon calculus exists which satisfies t-channel partial wave unitarity.

The generalization to more general multiparticle amplitudes is now rather straightforward. The crucial step in each case is that one first has to find the necessary decomposition of the amplitude, before one is able to write a multiple dispersion relation for the amplitude or a reggeon calculus for the partial wave functions.

In Fig.7 this decomposition is illustrated for the two sixpoint amplitudes  $T_{2 \rightarrow 4}$  and  $T_{3 \rightarrow 3}$ ; it holds in the kinematic region where all energy variables are as large as possible and the momentum transfers and Toller angles kept fixed. A more detailed discussion of these amplitudes (in particular certain subtleties connected with the last two terms in the decomposition of  $T_{2 \rightarrow 4}$  and  $T_{3 \rightarrow 3}$ ) can be found in Ref. 21.

As it can be seen from these few examples, the number of terms in the decomposition grows rather fast as the number of external particles increases. In practical calculations, however, it seems not necessary to

$$disc_j F(\delta, t) = \text{diagram with wavy line and two vertices (+ and -)} + \dots \quad (3.4)$$

("+" and "-" now refer to the j-variable). Together with

$$disc_j = \text{diagram with wavy line and two vertices (+ and -)} \quad (3.5)$$

and

$$disc_j = \text{diagram with wavy line and two vertices (+ and -)} \quad (3.6)$$

one has a coupled set of "partial wave" unitarity equations: this is the form in which t-channel unitarity enters the region  $s \rightarrow \infty, t \ll 0$ . In order to obtain a solution to these unitarity equations, it is sufficient that the partial wave function  $F(j, t)$  takes the form of a reggeon calculus. It is important to note that at this stage the parameters of the reggeon calculus (trajectory function, interaction vertices) may be rather general: t-channel unitarity alone requires only that the formal rules of the reggeon calculus are satisfied (presence of signature factors etc.).

We now come to the simplest case of an inelastic amplitude:  $T_{2 \rightarrow 3}$  in the double Regge region (Fig.5). Before statements analogous to (i)-(iii) of  $T_{2 \rightarrow 2}$  can be made for  $T_{2 \rightarrow 3}$ , we have to use one of the key results on the analytic structure of multiparticle amplitudes. It says that the amplitude  $T_{2 \rightarrow 3}$  in the double Regge limit splits into two parts, one having energy discontinuities only in the variables s and  $s_{ab}$ , the other one in s and  $s_{bc}$  (see Fig.6). In the partial wave representation one has:

$$T_{2 \rightarrow 3} = \frac{1}{(2\pi i)^2} \iint d\delta_1 d\delta_2 \left[ s^{\delta_2} s_{ab}^{\delta_1 \delta_2} \sum_{\delta_1} \sum_{\delta_2} F_R + s^{\delta_1} s_{bc}^{\delta_2 \delta_1} \sum_{\delta_1} \sum_{\delta_2} F_L \right] \quad (3.7)$$

$$\sum_{\delta} = \frac{e^{-i\pi\delta} + \tau}{\sin\pi\delta}$$

$$\sum_{\delta_j'} = \frac{e^{-i\pi(\delta_j - \delta_j')}}{\sin\pi(\delta_j - \delta_j')} + \tau\tau'$$

(3.8)

go beyond the sixpoint amplitude: it is believed that these amplitudes already contain all the essential complications of the analytic structure of multiparticle amplitudes (note that some of these complications do not yet show up in  $T_{2 \rightarrow 3}$ : the five point amplitude is still "too simple"). Once the correct expression for these amplitudes has been found, it seems possible to generalize to higher order amplitudes.

#### B. $T_{n \rightarrow m}$ in the leading logarithmic approximation

The construction of the multiparticle amplitudes  $T_{n \rightarrow m}$  in the LLA which will be described in the following has first been started by the Leningrad group <sup>22)</sup> and then been carried through independently in Refs. 23 and 24. A summary of the Leningrad school calculations can be found in Ref. 24. I will not have the time to present calculations in detail but will concentrate on making the logic as clear as possible. I will use the notations of Ref. 21, and more details can be looked up there. The starting point is the computation of tree graphs for  $T_{n \rightarrow m}$  which, in the language of dispersion relations, serve as subtraction constants. For illustration consider the  $2 \rightarrow 2$  vector scattering amplitude in lowest order perturbation theory. There are seven Feynmann diagrams (Fig. 8), and one finds that some of them individually have a bad high energy behavior (e.g. they grow like  $s^2$ ). However, when the sum is taken over all diagrams, these unwanted terms cancel and the final result has the appealing form:

$$2 g^2 s \frac{1}{t - M^2} \cdot \text{helicity matrices} \cdot \text{group structure} \quad (3.9)$$

where the helicity matrices are constant (independent of  $s$ ). As a graphical notation for (3.9) we use the diagram on the rhs of Fig. 8. The fact that all (but one) Feynmann diagrams of this order are necessary for obtaining (3.9) illustrates the extensive cancellations between different contributions of perturbation theory which are typical for vector theories. For the next amplitude,  $T_{2 \rightarrow 3}$ , the number of Feynmann diagrams, which have to be taken into account in order to find the correct high energy behavior of the tree approximation, is already much larger. But the result is again simple (Fig. 9):

$$2 g^3 s \frac{1}{t_1 - M^2} \vec{\Gamma}(q_1, q_2) \frac{1}{t_2 - M^2} \cdot \text{helicity matrices} \cdot \text{group structure} \quad (3.10)$$

where the three component vector

$$\vec{\Gamma}(q_1, q_2) = (\Gamma_{\sigma} e^{\sigma_1}, \Gamma_{\sigma} e^{\sigma_2}, \Gamma_{\sigma} e^{\sigma_3}) \quad (3.11)$$

stands for the production vertex labelling the polarizations of the produced vector particle. It has a nontrivial dependence upon the momenta  $q_1, q_2$  ( $q_1^2 = t_1, q_2^2 = t_2$ ) and the Toller variable  $\eta = 54s^2 b_{\sigma} / s$ . For  $T_{2 \rightarrow 4}$  the result is shown in Fig. 10: it takes the form of a multiperipheral production amplitude, the production vertex being given by (3.11) <sup>21)</sup>.  $T_{3 \rightarrow 3}$  is obtained from  $T_{2 \rightarrow 4}$  by crossing one of the produced particles.

An elegant method for computing these tree approximations for general  $T_{n \rightarrow m}$  has been suggested by Lipatov <sup>23)</sup>. Writing down a t-channel dispersion relation (without subtraction constants), only the particle pole contributes to the tree approximation of  $T_{2 \rightarrow 2}$ , and for this only the on-shell vertex functions have to be computed. The result agrees with (3.9). For  $T_{2 \rightarrow 3}$  a double dispersion relation in  $t_1$  and  $t_2$  is needed which has to be saturated by the pole contributions. The only new element is the production vertex whose off-shell continuation follows from direct computation and the requirement of gauge invariance:

$$\Gamma_{\sigma}(q_1, q_2) \cdot (q_1 - q_2)^{\sigma} = 0 \quad (3.12)$$

Proceeding in this way it is possible to verify the results of Figs. 9, 10 and to show that for general  $T_{n \rightarrow m}$  the tree approximations always have this multiperipheral structure. Within this approach the Lagrangian is needed only for the calculation of vertices in the tree approximation: tree amplitudes are built up by means of t-channel dispersion relations.

In the next step these tree approximations will be "dressed", and this is done by using s-channel dispersion relations plus unitarity. The amplitudes  $T_{n \rightarrow m}$  in the LLA are then built up order by order perturbatively. As a result of this "dressing" procedure, the elementary exchanges of the tree approximation will be reggeized.

Let me illustrate how this happens. To order  $g^4$  one has the one loop contribution to  $T_{2 \rightarrow 2}$ . For this amplitude the dispersion relation is:

me, however, shortcut these calculations a little bit. I directly use the ansatz (3.7) and, anticipating the result that the singularities in  $j_1$  and  $j_2$  will be the poles belonging to the reggeizing vector particle, I simply write:

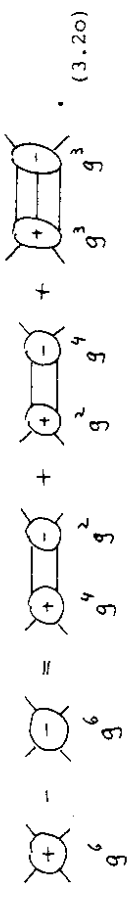
$$T_{2 \rightarrow 3} = S \sum_{\alpha_1, \alpha_2} s_{ab}^{\alpha_1 - \alpha_2} \sum_{\alpha_1 - \alpha_2} \overline{F}_R + S \sum_{\alpha_1, \alpha_2} s_{bc}^{\alpha_1 - \alpha_2} \sum_{\alpha_1 - \alpha_2} \overline{F}_L \quad (3.18)$$

(the functions  $\alpha_i = \alpha(t_i)$  should, of course, be the same as in (3.16)). The unknown quantities are now the coefficient functions  $F_L$  and  $F_R$ . For example, is determined by taking the  $s_{ab}$  -discontinuity of eq.(3.18), expanding in powers of  $g$ , and comparing the term  $g^5$  with the rhs of eq.(3.17). A consistency check can be made by taking the  $s$ -discontinuity of (3.18) and comparing it with the result of evaluating the unitarity equation which yields the  $s$  -discontinuity: both  $F_R$  and  $F_L$  in (3.18) are already fixed by the  $s_{ab}$  and  $s_{bc}$  discontinuities, resp., and no further freedom is left. What we have found in this way is that, up to this order of perturbation theory,  $T_{2 \rightarrow 3}$  is given by the exchange, in both the  $t_1$  and  $t_2$  channel, of the reggeized vector particle. This has to be compared with the tree approximation (Fig.9) where the exchanges are the elementary vector particles. In order to make this comparison more explicit (and also for later convenience), we rewrite eq. (3.18). Using the results for  $F_L$  and  $F_R$  (21), (3.18) can be written:

$$T_{2 \rightarrow 3} = 2 g^3 \frac{s_{ab}^{\alpha_1 - 1}}{t_1 - M^2} \overline{\Gamma}(q_1, -q_2) \frac{s_{bc}^{\alpha_2 - 1}}{t_2 - M^2} \times \text{helicity matrices} \times \text{group structure} \quad (3.19)$$

(where terms of the order  $g^5$   $\ln \frac{s_{ab} s_{bc}}{s}$  have been neglected). Eq. (3.19) is the form in which the double Regge exchange amplitude (Fig.11) would conventionally be represented: it is equivalent to (3.18), but it loses the information about the analytic structure in the energy variables.

In order  $g^6$  two contributions have to be calculated: the two-loop correction of  $T_{2 \rightarrow 2}$  and the one loop correction to  $T_{2 \rightarrow 4}$  ( $T_{3 \rightarrow 3}$ ). For  $T_{2 \rightarrow 2}$  we again use the dispersion relation (3.13). The unitarity equation for the discontinuity now has several contributions:



$$T(s, t) = a(t) + b(t) \cdot s + \frac{1}{\pi} \int_{s_0}^{\infty} ds' \frac{disc T(s', t)}{s'^2 (s' - s)} + \text{left hand cut} \quad (3.13)$$

The discontinuity follows from unitarity which, in this order of perturbation theory, has only the two-particle intermediate state:

$$disc T = \text{diagram with } + \text{ and } - \text{ signs} = \text{diagram with } + \text{ and } - \text{ signs} \quad (3.14)$$

On the rhs of this equation, only the  $2 \rightarrow 2$  amplitude to order  $g^2$  - which is the tree approximation - is needed: this we know from the first step of our calculations. Thus eqs. (3.13), (3.14) are sufficient to determine the leading term of  $T_{2 \rightarrow 2}$  in fourth order perturbation theory: the integral in (3.13) goes as  $s \ln s$  and, hence, dominates over the subtraction constants. The result is the term of the order  $g^4$  of the reggeizing vector exchange:

$$T_{2 \rightarrow 2} = -g^2 s^{\alpha(t)} \frac{e^{-i\pi \alpha(t)}}{t - M^2} \cdot \text{helicity factors} \cdot \text{group structure} \quad (3.15)$$

where

$$\alpha(t) = 1 + (t - M^2) g^2 \int \frac{d^2 k}{(2\pi)^2} \frac{1}{k_L^2 + M^2} \cdot \frac{1}{(q - k_L)^2 + M^2} \quad , \quad q_L^2 = -t \quad (3.16)$$

Comparison with the tree approximation (3.9) shows that the elementary exchange of (3.9) has been replaced by the reggeizing vector exchange.

In order  $g^5$  we have to calculate the one loop correction to the  $2 \rightarrow 3$  amplitude. In principle, we could proceed in the same way as we did for  $T_{2 \rightarrow 2}$ : one uses the decomposition of Fig.6 and writes down a double dispersion relation for each of the two terms, including the right number of subtraction terms. The various discontinuities and double discontinuities are computed via unitarity, for example:

$$disc_{s_{ab}} T_{2 \rightarrow 3} = \text{diagram with } + \text{ and } - \text{ signs} = \text{diagram with } + \text{ and } - \text{ signs} \quad (3.17)$$

On the rhs, only tree approximations are needed in this order of  $g$ . Let

On the rhs of this equation, all amplitudes are known from previous steps:  $T_{2 \rightarrow 2}$  in order  $g^2$  and  $g^4$ , and  $T_{2 \rightarrow 3}$  in the tree approximation. Inserting the result into the dispersion integral, we correctly reproduce the coefficient proportional to  $g^6$  of the amplitude (3.15).

The one-loop contribution to  $T_{2 \rightarrow 4}$  (and  $T_{3 \rightarrow 3}$ ) is obtained in the same way as for  $T_{2 \rightarrow 3}$ : to proceed most generally, one makes the decomposition (Fig.7) and writes a multiple dispersion relation for each term (with the right number of subtractions). Then unitarity equations are used for computing, in the given order, single and multiple discontinuities. But we again shortcut this procedure and make the ansatz analogous to (3.18). There are now five unknown coefficient functions which can be determined from the (single) discontinuities in the five subenergy variables. The discontinuity across the total energy  $s$  again serves as a consistency check. The result for  $T_{2 \rightarrow 4}$  can be written (Fig.12):

$$T_{2 \rightarrow 4} = 2 g^5 \frac{s_{ab}}{t_1 - M^2} \frac{\alpha_{1-1}}{\alpha_2-1} \frac{s_{bc}}{t_2 - M^2} \frac{\alpha_3-1}{\alpha_4-1} \frac{s_{cd}}{t_3 - M^2} * \text{helicity terms} * \quad (3.21)$$

\* group structure

and what we have just computed is the term  $g^6$  in the power series expansion of this equation. This result (Fig.12) is the "dressed" generalization of the tree approximation in Fig. 10.

This procedure of calculating order by order perturbation theory all multiparticle amplitudes  $T_{n \rightarrow m}$  in the LLA can be continued up to arbitrarily high order (in Ref.21, this has been done up to the order  $g^8$ ). Let me, however, stop already here and state the general result. For the four, five, and sixpoint amplitudes we have found that the  $T_{n \rightarrow m}$  have the simple multiregge form with only pole exchanges, and one should expect that this holds for general  $T_{n \rightarrow m}$  (Fig.13). This then generalizes the reggeization of the vector particle, as it was found already by Grisaru et al. 11) for  $T_{2 \rightarrow 2}$  on the level of the Born approximation. A nontrivial feature of this result is the fact that no Regge cuts appear: signature conservation rules would very well allow for two Regge cuts in the central rapidity gap of  $T_{2 \rightarrow 4}$  (Fig.12), but as a result of some subtle cancellations 21) these cut contributions drop out for the LLA. As we shall see later, such cut contributions will, however, come in when we go beyond this leading logarithmic approximation, requiring full s-channel unitarity.

One may ask how well justified our extrapolation from  $T_{2 \rightarrow 2}$ ,  $T_{2 \rightarrow 3}$ ,

$T_{2 \rightarrow 4}$ ,  $T_{3 \rightarrow 3}$  to general  $T_{n \rightarrow m}$  was. As a "proof" for the correctness of this generalization one can perform a consistency check and test the unitarity content of the  $T_{n \rightarrow m}$ : unitarity puts nonlinear constraints on the elements of the set  $T_{n \rightarrow m}$  which, on the level of the LLA, must be satisfied if our result is correct. For the simplest case,  $T_{2 \rightarrow 2}$ , it can, in fact, be shown 25) that the elements  $T_{2 \rightarrow 2}$  and  $T_{2 \rightarrow n}$  satisfy the "bootstrap" equation:

$$\text{disc}_s T_{2 \rightarrow 2} = \int_{-\infty}^{\infty} d\Omega_n \text{quantum number of the vector particle} \quad (3.22)$$

When "squaring", on the rhs of this equation, the  $T_{2 \rightarrow n}$  amplitudes, one has to take that quantum number configuration which corresponds to the exchange of the vector particle: from Fig.13 it is clear, that in the LLA all t-channels carry the quantum number of the vector particle and, in particular, there is no vacuum quantum number exchange yet. (For our SU(2) model we have, after the symmetry breaking due to the Higg's mechanism, a global SU(2) symmetry. If we call this symmetry, for the time being, isospin, then the vector particle carries the quantum number I=1. On the rhs of eq. (3.22) we then have the possibilities I = 0, 1, 2, and it is the I = 1 configuration that we must take).

For  $T_{2 \rightarrow 3}$  we have three constraints given by unitarity. In Ref.21 it is shown that the following relations hold:

$$\text{disc}_{s_1} T_{2 \rightarrow 3} = \int_{-\infty}^{\infty} d\Omega_n \text{quantum number of vector particle} \quad (3.23)$$

and

$$\text{disc}_s T_{2 \rightarrow 3} = \int_{-\infty}^{\infty} d\Omega_n \text{quantum number of vector particle} \quad (3.24)$$

quantum number of vector particle

but the quantum number of the vector particle in all exchange channels. This was because the leading power of lns in each order of perturbation theory always belongs to odd signature (the expansion of the signature phase factor  $(e^{-i\pi\alpha(t)} \pm 1)$  in powers of  $g^2$  starts with the constant  $-2$  for odd signature, but with  $O(g^2)$  for even signature). The requirement that the amplitude is odd under  $s \leftrightarrow u$  crossing projects out the quantum number of the vector particle.  $T^{(2)}$  therefore must contain even signature exchanges, in particular the Pomeron. The easiest way to find these amplitudes is via unitarity:

$$T^{(2)} - T^{(2)+} = 2 T^{(1)} T^{(1)+} + \int \text{even signature} \quad (3.28)$$

This defines  $T^{(2)}$ : on the rhs, at least one t-channel must have even signature, otherwise we would be back at eq. (3.26) and nothing new would have been found. Eq. (3.28) defines discontinuities; for obtaining the full amplitudes one uses the Sommerfeld-Watson representations, e.g. (3.7). The simplest example is  $T_{2 \rightarrow 2}^{(2)}$ . From (3.28) we have:

$$discs T_{2 \rightarrow 2}^{(2)} = \sum_n \int d\Omega_n |T_{2 \rightarrow n}|^2 \text{even signature} \quad (3.29)$$

This determines the partial wave of  $T_{2 \rightarrow 2}$  and is illustrated in Fig. 14. For one of the even signature channels, the Pomeron, the leading singularity in the j-plane comes out as a fixed cut <sup>25)</sup> to the right of  $j=1$ : it violates the Froissart bound and also dominates the LLA (3.15), both being a clear indication that the expansion (3.27) cannot be truncated after the first or the second term.

In case of the 2-3 amplitude the signature degree of freedom allows for three amplitudes contributing to  $T^{(2)}$ : the configurations  $(\tau_1, \tau_2) = (-,+), (+,+), (+,-)$ . For the first case a closer look at the signature factors (i.e. counting powers of  $g^2$  in eq. (3.81)) shows that, out of the two terms in the decomposition of  $T_{2 \rightarrow 3}$  (eq. (3.7) or Fig. 6), the second one which has the  $S_{6c}$ -discontinuity dominates over the first one. Hence, the amplitude can be constructed out of the  $S_{6c}$ -discontinuity alone:

$$discs S_{6c} T_{2 \rightarrow 3}^{(2)} = \sum_n \int d\Omega_n T_{2 \rightarrow n} \cdot T_{2 \rightarrow n}^+ / \text{even signature} \quad (3.30)$$

On the rhs of these equations the t-channel quantum numbers again have to be that of the vector particle. In the same way it can be shown that for  $T_{2 \rightarrow 4}$  and  $T_{3 \rightarrow 3}$  unitarity holds for all energy variables.

In order to summarize these unitarity properties of the  $T_{n \rightarrow m}$  in the LLA I use a matrix notation. Let  $T$  be the matrix whose elements are the  $T_{n \rightarrow m}$ :

$$T = \begin{pmatrix} T_{2 \rightarrow 2} & T_{2 \rightarrow 3} & \dots \\ T_{3 \rightarrow 2} & T_{3 \rightarrow 3} & \dots \\ \dots & \dots & \dots \end{pmatrix} \quad (3.25)$$

and let the subscript "1" remind us that we are dealing with the LLA. Then eqs. (3.22) - (3.24) are elements of the following matrix equation:

$$T^{(1)} - T^{(1)+} = 2i \cdot T^{(1)} T^{(1)+} \quad \text{quantum number (3.26) restricted}$$

On the rhs, all t-channels must have the quantum number of the vector particle. This restriction signals that  $T^{(1)}$  is not yet completely unitary: to find the missing pieces will be the task of the following subsection.

### C. Unitarization

In order to find a T-matrix which is fully unitary, i.e. satisfies eq. (3.26) without any restrictions on the rhs, we make the ansatz:

$$T = \sum_n T^{(n)} \quad (3.27)$$

with all the  $T^{(n)}$  being matrices of the form (3.25). The expansion parameter is the following.  $T^{(1)}$  is the LLA which has been obtained in the previous part; in the sense of the expansion in eq. (3.1) it represents the sum of the leading terms  $f_{n-1} (\epsilon_n s)^{n-1}$ .  $T^{(2)}$  is the sum of the next-to-leading terms, but as it was said in the beginning of this section, only those parts of the  $f_{n-2}$  will be found which are required by unitarity. Similarly,  $T^{(3)}$  corresponds to the  $f_{n-3}$ , etc.

To begin with the elements of  $T^{(2)}$ , we recall that  $T^{(1)}$  had nothing

In terms of reggeon diagrams, this equation is illustrated in Fig. 15. For the signature configuration (+, +), the  $g^2$ -expansion of the signature factors implies that the amplitude is proportional to its s-discontinuity:

$$T_{2 \rightarrow 3}^{(2)} \sim \text{disc}_s T_{2 \rightarrow 3}^{(2)} = \sum_n \int d\Omega_n T_{2 \rightarrow n} T_n \rightarrow 3 \left\{ \begin{array}{l} \text{even signature} \\ \text{odd signature} \end{array} \right. (3.31)$$

The reggeon diagrams for this amplitude are shown in Fig. 16.

The construction of  $T_{2 \rightarrow 4}$ ,  $T_{3 \rightarrow 3}$  proceeds in the same way. For the various signature configurations (-, -, +), (-, +, -), (+, -, -), (+, +, -), (-, +, +) (note that (+, -, +) does not belong to  $T^{(2)}$  but to  $T^{(3)}$ ), it is always sufficient to compute single discontinuities, and what one obtains are diagrams similar to Figs. 14-16. The following pattern then emerges for the elements of  $T^{(2)}$ : whereas the elements of  $T^{(1)}$  (Fig. 13) have always just one reggeon in the t-channel, those of  $T^{(2)}$  (Figs. 14-16) can have either one (for odd signature exchange) or two reggeons (for even signature exchange) in each t-channel. Since the rules, according to which the reggeon diagrams of Figs. 14-16 are constructed, agree with the general reggeon calculus for inelastic production amplitudes<sup>20</sup>, the elements of  $T^{(2)}$  also satisfy t-channel unitarity. The elements of this reggeon calculus (Fig. 17) are obtained from the defining equations (3.28), (3.29) (analytic expressions will be given in Ref. 26). To complete the construction of  $T^{(2)}$ , let me mention that also certain nonleading terms obtained from expanding the signature factors of the elements of  $T^{(1)}$  have to be counted as elements of  $T^{(2)}$ .

The construction of  $T^{(3)}$ ,  $T^{(4)}$ ... essentially repeats the steps which have led to  $T^{(1)}$  and  $T^{(2)}$ . At the level of  $T^{(3)}$  new contributions to the partial waves with only odd signature exchanges appear: this are reggeon diagrams involving the higher order 1-3 reggeon vertex (Fig. 18) or the one reggeon + three reggeons  $\rightarrow$  particle production vertex (Fig. 19). Compared to the diagrams of  $T^{(1)}$  (Fig. 3), these new contributions have two more powers of  $g^2$  (or, in other words, are down by two powers of  $\ln s$ ).

The lowest order (in powers of  $g^2$ ) contributions to Figs. 18 and 19 are shown in Fig. 20: these diagrams, having only elementary exchanges, are of the order  $g^6$ s and  $g^7$ s, respectively, and contain no logarithm of any energy variable. Furthermore, they are real. This implies that they cannot be obtained by just iterating s-channel unitarity (in the language of dispersion relations, they are subtraction constants), but

they must be computed by hand: going back to the Lagrangian, one has to use methods which are similar to those which were used for the tree approximations at the level of  $T^{(1)}$ . Details on this will be found in Ref. 27. To find the elements of  $T^{(3)}$ , one proceeds very much in the same way as we did for  $T^{(1)}$ : the lowest order elements (Fig. 20) play the same role as the tree approximations, and  $T_{2 \rightarrow 2}$ ,  $T_{2 \rightarrow 3}$ , ... are computed order by order perturbation theory by computing the energy discontinuities from unitarity equations (cf (3.14), (3.17), (3.20)). On the rhs of these equations, a careful counting of powers of  $g^2$  is needed, and contributions from  $T^{(1)}$ ,  $T^{(2)}$ , and  $T^{(3)}$  have to be taken into account. As a result of these calculations the elementary exchanges of Fig. 20 are "dressed", i.e. they are reggeized, and they also interact via the quartic reggeon vertex which was found in the previous step. The unitarity content of  $T^{(3)}$  is the following:

$$T^{(3)} - T^{(3) \dagger} = 2i \left[ T^{(1)} T^{(3) \dagger} + T^{(2)} T^{(2) \dagger} + T^{(3)} T^{(3) \dagger} \right] \quad (3.32)$$

odd signature

This is the analogue of eq. (3.26) for  $T^{(1)}$ . As in the case of  $T^{(2)}$ , also nonleading terms of  $T^{(1)}$  and  $T^{(2)}$  have to be counted as elements of  $T^{(3)}$ : they are obtained from expanding the signature factors in powers of  $g^2$ .

$T^{(4)}$  can be obtained from s-channel unitarity without computing new subtraction constants:

$$T^{(4)} - T^{(4) \dagger} = 2i \left[ T^{(1)} T^{(4) \dagger} + T^{(2)} T^{(2) \dagger} + T^{(3)} T^{(3) \dagger} \right] \quad (3.33)$$

even signature

In the matrixelements on the rhs, at least one t-channel must have even signature. Otherwise we would be back at (3.32). Eq. (3.33) is the analogue of (3.28) for  $T^{(2)}$ . The reggeon diagrams of  $T^{(4)}$  contain up to four reggeons in the t-channels.

Repeating these steps, higher and higher  $T^{(n)}$  are obtained: at each step the (maximal) number of reggeons in an exchange channel increases by one, and new elements (vertices with a nontrivial momentum dependence) appear. The result for  $T$  is a complete reggeon calculus, with the reggeizing vector particle being the reggeon and having (infinitely many) selfinteraction vertices. In principle all these vertices are calculable,



but so far only a few of them are known, and to find a simple expression for the most general  $n \rightarrow m$  reggeon vertex remains a subject of future work.

The fact that the result of our unitarization procedure comes in form of a complete reggeon calculus was to be expected as soon as the reggeization of the vector particle had been established. For future investigations it might, however, be useful to mention that, by a slight rearrangement in the expansion of  $T$ , a more physical picture of the (elastic) scattering process can be obtained. The idea is simply to reexpand each reggeon diagram in the expansion

$$T_{2 \rightarrow 2} = \sum_n T_{2 \rightarrow 2}^{(n)} \quad (3.34)$$

in powers of  $g^2/(j-1)$  (note that each reggeon line by itself represents a power series in this parameter:  $[j-1 - (\alpha(t)-1)]^{-1} = [j-1]^{-1} \sum_m \left(\frac{\alpha(t)-1}{j-1}\right)^m$ ) with  $\alpha-1 = O(g^2)$ :

$$T_{2 \rightarrow 2}^{(n)} = \sum_m \left(\frac{g^2}{j-1}\right)^m t_m^{(n)} \quad (3.35)$$

$(F_{2 \rightarrow 2}^{(n)})$  is the partial wave of the amplitude  $T_{2 \rightarrow 2}^{(n)}$ . Since the variables  $j-1$  and  $\ln s$  are conjugate to each other (cf. eq.(3.2)), (3.35) leads to an expansion of  $T_{2 \rightarrow 2}$  in powers of  $g^2 \ln s$  and has a physical interpretation close to that of the well-known multiperipheral model (for a description of these ideas see Ref.27). The term proportional to  $(g^2 \ln s)^m$  represents the following subprocess of elastic scattering: out of the incoming fast hadron which is a composite system of virtual constituents (partons), some parton has initiated a  $m$ -step cascading decay. At the end of this decay slow partons (wee partons) have been produced which can interact with the target at rest. This process is illustrated in Fig.21. In the introduction I raised the question whether the hadron radius can be made finite: this means that we are interested in the distribution of these wee partons in impact parameter space. As I will explain a little later, the expansion (3.35) may be a better starting point for investigating this question than the reggeon calculus representation of the  $T$ -matrix that was obtained in the first instance. This is the reason why I mentioned this second form of representing the matrix  $T$ .

#### D. The zero mass limit

In the first three parts of this section I have been dealing with the question of how to select those terms in the perturbation expansion which are needed for obtaining a reliable high energy description. All this was done for the massive  $SU(2)$  Higg's model, but our final aim is the pure Yang-Mills case. We therefore have to investigate how our  $T$ -matrix behaves under the limit which takes us from the Higg's model to the pure Yang-Mills case.

The  $T$ -matrix whose construction I have outlined before depends only on the two parameters  $g$  (the gauge coupling) and the mass of the vector particle  $M^2 = g^2 \mu^2 / \lambda$  (cf. eq.(2.10)), but not on the Higg's parameters  $\mu$  and  $\lambda$  separately. For our purposes it is, therefore, sufficient to demand that  $M^2 \rightarrow 0$ ,  $g$  staying fixed. A brief investigation of low order perturbation theory shows that, in order to decouple the Higgs sector from the gauge particles, one should take  $\lambda$  and  $\mu$  to infinity such that  $\mu^2/\lambda \rightarrow 0$ . For the time being, I shall concentrate on the question how our  $T$ -matrix behaves when  $M^2$  is taken to zero. But it seems to me that a more accurate study of the transition from the Higgs model to the pure Yang-Mills case would be very desirable.

First it is necessary to replace the external states which so far have been taken to be massive vectors and scalars. It is wellknown from QED calculations<sup>28)</sup> that the simplest case of a high energy scattering amplitude which is finite in the zero mass limit of the photon is that of elastic photon-photon scattering (or elastic photon-electron scattering): the incoming photon dissociates into a electron-positron pair which interacts with the target via photon exchanges (note that elastic electron-electron scattering via multiphoton exchange is not infrared finite). This can easily be generalized to the nonabelian case<sup>24)</sup> (Fig. 22a): replace the external photons by hadrons, say vector mesons with some wave functions, and take the fermions to be quarks. It can then be shown<sup>26)</sup> for  $T_{2 \rightarrow 2}^{(2)}$ , the first term in the expansion (3.27) which contributes to elastic scattering, that in the zero quantum number exchange channel the limit  $M^2 \rightarrow 0$  exists and is finite to all orders of  $g^2$ . For higher terms in (3.27),  $T_{2 \rightarrow 2}^{(4)}$  etc., this can be shown<sup>26)</sup>, so far, only for important subsets of terms (for example those shown in Fig.22b); but from the results of studying infrared singularities in hard scattering processes<sup>29)</sup> it seems likely that in the vacuum quantum number (color zero) channel infrared singularities should always cancel.

Let me assume that this, in fact, is true for all the  $T^{(n)}$  in (3.27). Then our present situation can be described as follows (Fig. 23). Starting again from the deep inelastic region where the use of perturbation theory (and in this case even the summation of only leading logarithms) rests on a safe ground, we now have isolated those Feynmann diagrams which have to be summed when the Regge limit is taken ( $q^2$  fixed and  $x \rightarrow 0$ ). They are obtained as the zero mass limit of our  $T$ -matrix which is coupled to the quark loop as external source.

I finish this long section with a few comments on other approaches to the same problem. When describing the derivation of the LLA, I have restricted myself to that method which, as I believe, is most suitable for achieving unitarity: the use of the analytic structure of multiparticle amplitudes together with unitarity. Other groups of authors<sup>30) 31)</sup> have followed the more conventional method of investigating Feynmann integrals and extracting the leading term by use of a clever choice of integration variables. This approach has so far been restricted to the  $2 \rightarrow 2$  amplitude (with one exception<sup>32)</sup>) in the LLA and one step beyond (in our notation:  $T_{2 \rightarrow 2}^{(2)}$ ). Wherever a comparison can be made, the results of the different approaches agree. As to the next logical step, namely the unitarization of the LLA, Refs. 33 and 34 claim that the fully unitary  $S$ -matrix takes a simple eikonal form, both for QED and the nonabelian case. However, when reexpanding this eikonal representation, it appears that pieces are missing which are necessary for having  $s$  and  $t$ -channel unitarity. From the  $s$ -channel point of view, subchannel unitarity is not satisfied, i.e. rescattering contributions to inelastic production amplitudes are missing.  $T$ -channel unitarity (partial wave unitarity) requires that the lowest order  $g^2$ -expansion coefficients of the 3-reggeon, 5-reggeon, ... cut diagrams are real. Hence, they cannot be obtained from iterating  $s$ -channel unitarity alone, as it is done in the eikonal expression of Ref. 34.

A very different approach has been taken in Ref. 35. For the case of quark-quark scattering, the leading infrared divergent terms are isolated by means of the equations of Cornwall, Tictopoulos and Korshaus-Altes, de Rafael, and then the behavior of these terms in the Regge limit is studied. The result is a fixed cut singularity at  $j=1$ . Compared to the procedures which I have been describing so far, this amounts to taking the two limits (Regge limit  $s \rightarrow \infty$  and zero mass limit  $M^2 \rightarrow 0$ ) in the reverse order. As it has been shown by Bronzan and Sugar<sup>36)</sup>, these two limits do not commute: the terms found in Ref. 35 (first  $M^2 \rightarrow 0$ , then  $s \rightarrow \infty$ ) form a subset of those obtained from the other approach (first

$s \rightarrow \infty$ , then  $M^2 \rightarrow 0$ ) and, hence, do not seem to satisfy unitarity.

## IV. Summation of the diagrams

I now come to the final part of my talk: how can one try to sum all the contributions that have been obtained in the previous section? Let me recall the two quantities we wanted to concentrate on: the  $s$ -dependence of the total cross section as the most important observable, and the hadronic radius  $\langle b^2 \rangle$  as a test for the reliability of the calculations. Unfortunately, I will not be able yet to give you final answers. The task of summing all these contributions of  $T$  (or, at least, of extracting the relevant information about the leading  $s$ -behavior) requires new techniques, and all I can do is to outline the main ideas and mention those results which we already have. For the investigation of the two quantities  $\langle \sigma_{tot} \rangle$  and  $\langle b^2 \rangle$  two different approaches seem to emerge: the first one starts from the reggeon calculus representation of the  $S$ -matrix and then makes use of the phase structure of reggeon field theory which has been studied within the last few years. For a study of the parton distribution in  $b$ -space, on the other hand, the power series (3.35) seems to be a good starting point, and I would like to begin with this approach first.

To be specific, let us consider the model illustrated in Fig. 22 (elastic scattering of two  $q\bar{q}$  bound states via gluon exchanges), assuming that the zero mass limit exists for all  $T_{2 \rightarrow 2}^{(n)}$  in the vacuum exchange channel. As explained before, the expansion in powers of  $g^2 \mathcal{L}_{ns}$  (c.f. (3.35)) can be related to the parton picture: each power of  $g^2 \mathcal{L}_{ns}$  stands for a change in rapidity by one unit, and the term  $(g^2 \mathcal{L}_{ns})^m t_m$  corresponds to a  $m$ -step decay of some fast constituent into slower ones such that at the end we have partons emerge. For the rest frame of the target, this situation is illustrated in Fig. 21, for the CM-system in Fig. 24: each horizontal line denotes a point in rapidity (i.e. all points on one line have the same rapidity), but each vertex has its own impact parameter coordinate. The (statistical) distribution of all these points in impact parameter space defines the extension of the hadron. For the lowest approximation to the elastic scattering process,  $T_{2 \rightarrow 2}^{(2)}$ , there is a direct analogy to Figs. 21 (or 24): two successive steps in the expansion (3.35) are connected by a single two-dimensional transverse momentum integration, i.e.  $t_{m+1}^{(2)} = K \cdot t_m^{(2)}$  with  $K$  being an integral operator (the explicit form of this recursion relation can be found in Ref. 25) or  $t_{m+1}^{(2)} = K \times K \times \dots \times K \times t_1^{(2)}$ . The lines in Fig. 24a then denote the flow of transverse momentum in  $T_{2 \rightarrow 2}^{(2)}$ . At the level of  $T_{2 \rightarrow 2}^{(4)}$ , the momentum flow becomes more complicated (Fig. 24b): between two rungs there

may be more than two vertical lines, since the kernel in  $t_{m+1}^{(4)} = K \cdot t_m^{(4)}$  involves more than one  $K_I$ -integral. With increasing  $n$  the number of vertical lines (i.e. the number of  $K_I$ -integrations in  $T_{2 \rightarrow 2}^{(n)}$ ) increases, giving rise to more and more interaction between partons of different rapidity.

In order to study the  $b$ -distribution of the partons in Fig. 24 we shall investigate how the leading  $j$ -plane singularity of the partial wave in (3.35) is generated (i.e. we study the behavior of the expansion near the rightmost value of  $j$  for which the series diverges). For this we use an observation made by Kuraev et al. 25) for the case of  $T_{2 \rightarrow 2}^{(2)}$ : the divergence of the expansion

$$T_{2 \rightarrow 2}^{(2)} = \sum_m \left( \frac{g^2}{g^2 - 1} \right)^m t_m^{(2)} \quad (4.1)$$

comes from a specific region of phase space of the  $k_I$ -integrations in Fig. 24a. Each  $K_I$ -integration is perfectly finite, but for large  $m$  (which is the number of rungs or cells in Fig. 24a) the dominant region of integration in those cells which are far away from the external particles moves more and more towards large  $k_I$ -values:

$$\langle \mathcal{L}_n k_I^2 \rangle = c_2 \sqrt{m} \quad (4.2)$$

where  $c_2$  is a computable number (note that this type of growing transverse momentum is quite different from that found in hard scattering processes). Eq. (4.2) means that the average value of  $\mathcal{L}_n k_I^2$  obeys a diffusion law as a function of the number of steps. Once  $k_I^2$  is large, the resulting singularity will not depend on finite quantities such as the mass  $M^2$  or the momentum transfer  $q^2 = -t$ : this explains its nature of being a fixed cut. The  $j$ -value  $j_c$  for which this singularity arises lies to the right of  $j = 1$  and leads to a total cross section which grows like  $\sigma_{tot} \sim s^{j_c - 1}$  (Fig. 25a). Since with (4.2) also  $\langle k_I^2 \rangle$  grows, as the number of steps  $m$  increases, the variable  $b^2$  conjugate to  $k_I^2$ , which stands for the distance in impact parameter between neighboring vertices in Fig. 24, becomes smaller and smaller, and the parton distribution inside the upper (or lower) hadron is of the form shown in Fig. 25b. As to the zero mass limit  $M^2 \rightarrow 0$ , the most interesting point is that of  $q^2 = -t = 0$  24): the large  $b$ -behavior comes from the small  $q_I$ -region. For  $M^2 = 0$ ,  $q^2 = 0$  the diffusion picture of  $\mathcal{L}_n k_I^2$

still holds, but  $\langle \mathcal{L}_n k_L^2 \rangle$  now moves in both positive and negative direction:

$$\langle \mathcal{L}_n k_L^2 \rangle = \pm c_2 \sqrt{m} \quad (4.3)$$

( $c_2$  being independent of  $M^2$  is the same as in the massive case (4.21)). In b-space the large negative values of  $\langle \mathcal{L}_n k_L^2 \rangle$ , i.e. the small values of  $k_L^2$ , allow for longer and longer steplengths in b-space, and the radius  $\langle b^2 \rangle$  grows too fast (as a power of s). This implies that, at the level of the approximation  $T^{(2)}$ , (a) the radius  $\langle b^2 \rangle$  is too large, and (b) the limit  $M^2 \rightarrow 0$ , although it exists order by order perturbation theory, is discontinuous for the leading s-behavior. The last point has been made explicit<sup>24</sup> by solving at  $t=0$  the integral equations of  $T_{2 \rightarrow 2}^{(2)}$  for  $M^2 \neq 0$  and for  $M^2 = 0$ : there is a jump in the s-behavior of  $\mathcal{G}_{t \rightarrow t}^{(2)}$  at the point ( $M^2 = 0, t = 0$ ), compared to  $M^2 \neq 0$  and / or  $t \neq 0$ .

As a guideline to what the situation in a realistic high energy theory should be, it might be useful to recall a few features of the multiperipheral model. Writing the amplitude in the form (4.1), one finds that  $t_m \sim [\beta(t)]^m$  with  $\beta(t)$  being the integral in equation (3.16), and the resulting j-plane singularity is a moving pole. Since the  $k_L$ -integrations in  $[\beta(t)]^m$  are always superconvergent, and their mean values do not depend on m at all, the average steplength in b space is constant, and we have the well known random walk picture in b-space with  $\langle b^2 \rangle \sim \alpha' \mathcal{L}_n s$ . This suggests that in our nonabelian gauge theory model we should look for a mechanism which stops the growth of  $\langle k_L^2 \rangle$  as a function of the number of steps.

Let me briefly outline<sup>37</sup> how the presence of the higher  $T^{(n)}$  could lead to a change in the right direction (as long as one does not know the form of general  $T^{(n)}$  in full detail I can describe this only qualitatively). A simple dimensional argument for the general  $n \rightarrow m$  reggeon vertex shows that the diffusion law (4.2) for  $\mathcal{L}_n k_L^2$  will always hold, provided the limit  $M^2 \rightarrow 0$  is finite. The only new feature compared to  $T_{2 \rightarrow 2}^{(2)}$  is that the momentum integration between two steps in Fig. 24b now may consist of two or more  $k_L$ -loops, and the variable which grows is the mean value of these  $k_L^2$ :

$$\mathcal{L}_n k_L^2 = \frac{1}{n} [\mathcal{L}_n k_{L1}^2 + \dots + \mathcal{L}_n k_{Ln}^2] \sim c_n \sqrt{m} \quad (4.3)$$

or

$$k_L^2 = \sqrt{k_{L1}^2 \cdot k_{L2}^2 \cdot \dots \cdot k_{Ln}^2} \quad (4.4)$$

The numbers  $c_n$  in (4.3), belonging to the approximation  $T^{(n)}$ , will be different from  $c_2$  in (4.2): if the growth of  $\mathcal{L}_n k_L^2$  should come to a stop, we must have  $c_n \rightarrow 0$  as  $n \rightarrow \infty$ . The situation of the n variables  $\mathcal{L}_n k_L^2$ , whose "center of mass" coordinate obeys the diffusion law, resembles that of the one-dimensional motion of n atoms, moving in a potential which depends only on the relative distance of the atoms from each other, but not on the center of mass position. In such a case the center of mass coordinate obeys the diffusion law, and depending on whether the relative forces between the atoms are attractive or repulsive the diffusion will be slower or faster than in the absence of those forces. The crucial observation now is that, if the forces are sufficiently attractive, the motion of the center of mass can come to stop when the number of atoms becomes infinite. Applying these ideas to our  $T^{(n)}$ , we see that if the number of  $k_L$ -variables in (4.4) becomes very large - i.e. in Fig. 24 there is more and more interaction between different horizontal lines, each of which represents a certain rapidity in the "gluon cloud" around the incoming hadron - the growth of  $k_L$  towards the center of Fig. 24 can come to a stop, and the impact parameter steplength stays finite and constant. About the s-dependence of  $\mathcal{G}_{t \rightarrow t}^{(n)}$  very little can be said as long as this argument has not been made quantitative yet: if the series of the  $T^{(n)}$  converges, the cross section (Fig. 25a) must flatten out at high energies in order to satisfy the Froissart bound.

It is important to mention that the same type of analysis has also to be carried out for the abelian case of QED. At the level of the LLA for the Pomeron channel, the leading singularity of the tower diagrams (38), (39) in QED is also a fixed cut to the right of  $j=1$  and has very much the same characteristics as in the nonabelian case. Important differences between the two cases are expected to come in when the effects of the higher approximations  $T^{(n)}$  are included (it seems that the sum of all those diagrams which are described in Ref. 38 and Ref. 40 for QED represents the analogue of the  $T$  that we have discussed for the nonabelian case. The eikonal graphs of Ref. 39 and even the "operator eikonal" expansion of Ref. 33 only form a subset of the more general class of diagrams in Refs. 38 and 40 and do not satisfy full s-channel unitarity).

Let me now describe the other approach towards analyzing the structure of  $\tau$  that I mentioned at the beginning of this section. It starts from the reggeon calculus representation of  $\tau$  and then uses the phase structure of reggeon field theory (RFT) which has been investigated during the last years. As it is well-known<sup>3)</sup>, RFT lives in two space and one time dimension (impact parameter and rapidity), and it has a nonrelativistic energy-momentum relation:  $E = \Delta + \alpha' K_{\perp}^2$  ( $E=1-j$ ,  $j$  = angular momentum;  $\Delta = 1 - \alpha(0)$ ;  $\alpha(0)$  and  $\alpha'$  are intercept and slope, respectively, of the trajectory function). This it is quite different from relativistic quantum field theory, and since, moreover, the triple interaction vertex (at least for the Pomeron case) is purely imaginary, it is clear that the phase structure of RFT, as a function of the "mass"  $\Delta$ , is not the same as in usual quantum field theory models. It will, therefore, be useful to first review what we know about the phases of RFT. As I have said in the beginning, RFT is designed to satisfy t-channel unitarity (to be more precise: partial wave unitarity), and, there is no a priori restriction on the parameters such as  $\Delta$  and  $\alpha'$ : as long as no connection was made between RFT and a specific underlying theory, it was, therefore, the strategy to vary the RFT parameters and to see for which values a realistic strong interaction theory emerges.

Fig. 26 shows the two phases of RFT: the intercept of the output singularity, i.e. the power of  $s$  of the elastic forward scattering amplitude, has been plotted as a function of the negative bare mass:  $-\Delta_0 = \alpha(0) - 1$ . In the subcritical phase to the left of the dotted line the total cross section is falling. There is no problem with s-channel unitarity, but from the physical point of view this phase has little interest, since in nature  $\sigma_{tot}(s)$  is far from being falling. When  $-\Delta_0$  approaches the critical value slightly to the right of zero (i.e.  $\alpha_{sc}(0)$  is slightly above one), the total cross section becomes less and less falling until the power of  $s$  reaches zero: at the critical point  $\sigma_{tot}(s) \sim (\ln s)^{-1}$ ,  $\gamma \sim 0.2$ . At this critical point a phase transition occurs: particle production shows long range correlations, and for the elastic scattering amplitude a scaling law with two anomalous dimensions holds. Consistency of this solution with s-channel unitarity is highly nontrivial: it has been checked quite extensively (including the decoupling problems of the Pomeron), and all tests have been passed successfully. Thus this critical RFT is an excellent candidate for strong interaction theory at high energies. Those energies, however, for which asymptopia of strong interactions is expected to set in, lie above presently available energy ranges, and it remains to explain how the finite energy tail of asymptopia connects up with critical RFT. In the supercritical phase to the right of

the dotted line in Fig. 26 (the bare mass is now negative) two solutions have been suggested (and there is still disagreement on which of them is the correct one): the first one has been obtained by Amati et al<sup>41)</sup> and leads to a total cross section which saturates the Froissart bound  $\sigma_{tot}(s) \sim (\ln s)^2$ . For such a behavior of the total cross section unitarity in the s and t-channel presents certain problems, and a complete check is still missing. The most important physical implication of this solution lies in the fact that the rise of the total cross section as observed at ISR energies, does not require any special value for  $\Delta_0$ : as long as  $\Delta_0 < \Delta_0^{critical}$ , the behavior of  $\sigma_{tot}(s)$  has the same s-dependence. The other solution to RFT in the supercritical phase has been presented by A. White<sup>42)</sup>. It leads to a falling total cross section, thus making the phase picture in Fig. 26 quite symmetric with respect to the critical point. While this solution has no problems with unitarity, its physical implications are very strong: the only possibility for having a nonfalling total cross section is critical RFT, and this requires a very special reason why the bare Pomeron intercept takes just the critical value. White<sup>43)</sup> also gives an explanation for this: he argues that criticality of RFT can be explained within QCD as being equivalent to confinement. I shall now try to explain this argument, which, of course, relies upon the validity of the second solution to supercritical RFT. However, I should emphasize once more that several people consider the first solution to be the correct one.

The basic idea is this: one reformulates the reggeon calculus (which has been derived in the previous section and, as elementary reggeon, only contains the quantum number carrying vector particle but no Pomeron), in terms of a new RFT which now contains, in addition to the vector particle reggeon field, also a Pomeron field (in terms of the vector particle, the Pomeron is a bound state of an even number of vector particles). Then one investigates the structure of this RFT as a function of the parameters of the Yang-Mills theory, in particular the mass  $M$  of the vector particle. For the Yang-Mills theory at  $M^2 \neq 0$  (one now considers generalizations of the SU(2) Higg's model: the gauge group could be SU(3), and the pattern of generating masses for the vector particles may be more complex), it is argued that the normal i.e. -prescription should be replaced by a principal value regularization: by assumption, this is the way to reach, in the limit  $M \rightarrow 0$ , the pure Yang-Mills case in the confining phase. The RFT obtained from such a modified Yang-Mills is found to be in the supercritical phase with a falling cross section, as long as  $M^2 \neq 0$ , and it becomes critical at  $M^2 = 0$ . As a result, the

nonfalling cross section, being a very special feature of strong interaction physics, can be explained only in a massless confining vector theory, where confinement, by assumption, is reached in the zero mass limit of massive Yang-Mills theory with a modified  $i\epsilon$ -prescription.

In order to explain this argument in somewhat more detail, it will be necessary to say a few more words about the solution to supercritical RFT, as it has been obtained before any connection to an underlying theory was made. Let us start with a RFT that contains, as the only field, the Pomeron in the subcritical phase, and decrease the mass from positive values to negative ones. Beyond the critical point the effective potential (for simplicity, our RFT contains only a triple interaction) has its stable minimum no longer at the origin, and by redefining the field variables one has to expand around other field configurations (note that in contrast to, say, the simplest Higgs model one cannot simply perform a shift of the field variables by a constant (i.e. time independent) amount: a detailed description of the "generalized shifting" procedure can be found in Ref.42). As a result, new interaction terms (Fig. 27a) and new diagrams (Fig.27b) appear, involving creation and annihilation of Pomeron pairs out of the vacuum, and the mass of the Pomeron propagator is positive again. The "new" elements in Fig. 27a, b lead to additions to the triple Pomeron interaction (Fig. 27c), giving rise to a nontrivial momentum dependence. In fact, this momentum dependence is singular: the reggeon line inside the vertex of Fig.27c carries a factor  $[\alpha_0' t_1 - |\Delta_0 - \Delta_{oc}|]^{-1}$  which for positive  $t_1$  produces a pole. This singularity is of the same form as if the upper reggeon in Fig. 27c would be an odd-signature massive vector particle of mass  $|\Delta_0 - \Delta_{oc}|$ , accompanied by its signature factor  $[\cos \frac{\pi}{2} \alpha(t_1)]^{-1}$ : this suggests that the supercritical phase has a more complex reggeon content than the subcritical phase we started with. A more detailed investigation (which, via cut reggeon field theory, takes into account the s-channel unitarity content of RFT) shows, in fact, that a consistent interpretation of this solution of supercritical RFT requires the presence of several massive reggeizing vector particles in addition to the Pomeron: in Fig. 27b, for example, the two-reggeon intermediate state receives contributions from both the two-Pomeron cut and the two vector particle cut. At the critical point  $\Delta_0 = \Delta_{oc}$  these vector particles become massless (together with the Pomeron), but they completely decouple from the Pomeron because the vertices in Fig.27a are proportional to  $\Delta_0 - \Delta_{oc}$ .

In the next logical step of the argument one wants to identify these massive vector particles with massive gluons that exist in an unconfined phase of Yang-Mills theories (QCD). For this it is necessary to show how the (massive) reggeon calculus of the previous section (the SU(2) Higgs model now being generalized to other gauge groups and Higg's patterns) can be mapped into such a supercritical RFT. Let me show, as an example, that with an appropriate definition of the Pomeron certain elements of the reggeon calculus have, in fact, the same structure as the "singular" RFT vertex of Fig. 27c. One of the simplest elements of the reggeon calculus, the  $2 \rightarrow 2$  reggeon vertex, consists of several contributions one of which is illustrated in Fig. 28. Its momentum dependence comes from the exchange of an elementary gluon between the two reggeized gluons. Each reggeon line in Fig. 28a carries its signature factor which, in the small  $g$  approximation is simply a propagator  $[\epsilon - M^2]^{-1}$ . The singularity structure of the two-reggeon state to the left of the interaction vertex is easily analyzed: besides the two-reggeon cut, there is the reggeon particle singularity which for the normal  $i\epsilon$ -prescription sits on an unphysical angular momentum sheet, and the two-particle cut. Now it becomes crucial to modify the  $i\epsilon$ -prescription such that the reggeon particle singularity appears on the physical sheet (simultaneously the two-particle cut disappears on the unphysical sheet): in the limit  $M \rightarrow 0$  it becomes a pole degenerate with the Regge pole of the vector particle, but it still has the quantum numbers of a bound state of two gluons and can be identified as the Pomeron singularity. Taking this singularity on the lhs in Fig.28a and drawing a single Pomeron line for this bound state of a reggeizing gluon and an elementary gluon, we arrive at Fig.28b which (always in the limit  $M^2 \rightarrow 0$ ) is of the same form as Fig. 27c. This shows that a certain part of the reggeon calculus has, after changing the  $i\epsilon$ -prescription, the same structure in angular momentum and transverse momentum as supercritical RFT. In the same way more complicated parts of the reggeon calculus can be identified with higher order elements of RFT in the supercritical phase. It is, however, clear that this way of dividing the reggeon calculus of massive Yang-Mills theories into several pieces each of which goes into different elements of the RFT raises counting problems which still remain to be solved: before this can be done it will be necessary to complete the calculation of the most general element of the reggeon calculus which has not been found yet.

Finally, the limit  $M^2 \rightarrow 0$  is taken and by assumption, massive Yang-Mills theory with the modified infrared regularization reaches QCD in the

## IV. Summary: the Regge limit in QCD

In these lectures I have reviewed the present status of the high energy (Regge) limit of nonabelian gauge theories, distinguishing between what has been achieved already, what sort of strategies and approaches seem to emerge, and what remains to be done in the future. Since (almost) all existing calculations start from perturbation theory of spontaneously broken gauge theories, hoping that at the end the limit, where the Higgs sector decouples, can be taken and reaches pure Yang-Mills theory, I have first tried to illustrate how good perturbation theory can be for this Regge limit: there is hope that perturbation theory is a valid starting point, since the Regge limit can be studied very close to the perturbative regime of QCD. But selection and summation of terms in the perturbation expansion must be much more complicated, because the Regge limit is also sensitive to features that have to do with confinement. It is, therefore, necessary to keep a certain control, throughout all calculations, of how reliable the perturbative approach is, and this can be done by keeping an eye on the hadron radius  $\langle b^2 \rangle$ .

After dividing gauge models into two classes - those where all vector particles reggeize and those where some of them don't - I have spent some time on describing, for the first type, how unitarity in both the s and t-channel can be used to classify those terms in the perturbation expansion which (at least) have to be summed up for obtaining a valid high energy description. The result (for the massive, i.e. spontaneously broken, Yang-Mills case) comes in form of a complete reggeon calculus, thus generalizing that property of the theory which at a lower level had manifested itself in the reggeization of the vector particles. The elements of this reggeon calculus are computable, but an expression for the general interaction vertex has still to be found. The zero-mass limit seems to exist, provided the external couplings are taken to be a model for hadronic bound states (e.g.  $q\bar{q}$ ).

For the summation of all these contributions two different approaches seem to emerge. The first one, being more geometrical, investigates the distribution in impact parameter space of the wee partons. A diffusion picture then emerges which is quite different from the random walk picture in multiperipheral models: diffusion, as a function of the number of steps, takes place in the variable  $\langle n K_1^2 \rangle$  rather than b. It is argued that, after summing all contributions required by unitarity, the hadronic radius  $\langle b^2 \rangle$  may stay finite when the mass of the vector particles is taken to zero, but a new technique has to be developed

confining phase. At the same time, the masses of the KFT elements, being of the order  $M^2$ , approach zero, and the singular elements à la Fig. 28b disappear: from the analysis of the supercritical phase of RFT it then follows that the KFT has become critical with the nonfalling cross section  $\sigma_{tot} \sim [\ln s]^{-\nu}$  (44).

in order to put this on a firm ground. Such a technique would also allow to study the abelian case (QED), where the summation of diagrams is still incomplete. The second approach makes use of the phase structure of reggeon field theory, and is based upon one of the two competing solutions that have been advocated for the supercritical phase. By assuming that QCD in the confining phase can be reached from spontaneously broken gauge theories in the zero mass limit, but only after the  $1\epsilon$ -prescription of the massive case has been altered, it is argued that such a massive case corresponds to supercritical reggeon field theory with a falling cross section, whereas in the zero mass limit the reggeon field theory becomes critical with the nonfalling cross section  $\sigma_{tot} \sim (k_{MS})^{-\delta}$ .

Acknowledgement:

For very helpful discussions I am indebted to Profs. V.N.Gribov, L.N.Lipatov and A.R. White.

Figure captions

- Fig.1 : Hadronic part of the deep inelastic leptonproduction process in QCD
- Fig.2 : Simplest model for elastic photon-hadron scattering in QCD: the sum goes over all possibilities of coupling two gluons to the quark lines
- Fig.3 : Reggeization of an elementary particle in field theory: the exchange on the lhs is elementary, on the rhs the particle reggeizes
- Fig.4 : Model for the Pomeron in QCD: the lhs denotes the unitary high energy expression for vector-vector scattering in the massive Higgs model; on the rhs the external particles are replaced by  $q\bar{q}$  bound states, and the gluon mass is taken to zero
- Fig.5 : Kinematics of the  $2 \rightarrow 3$  process in the double Regge limit
- Fig.6 : Analytic decomposition of the  $2 \rightarrow 3$  amplitude in the double Regge limit
- Fig.7 : Analytic decomposition of the  $2 \rightarrow 4$  and  $3 \rightarrow 3$  amplitudes
- Fig.8 : Seven Feynmann diagrams for vector-vector scattering in lowest order perturbation theory and their high energy behavior
- Fig.9 : High energy behavior of the  $2 \rightarrow 3$  process in the tree approximation
- Fig.10 : High energy behavior of the  $2 \rightarrow 4$  process in the tree approximation
- Fig.11 : The leading-logarithm approximation of  $T_{2 \rightarrow 3}$ : the wavy lines denote the exchange of a reggeized vector particle
- Fig.12 : The leading-lns approximation of  $T_{2 \rightarrow 4}$
- Fig.13 : The leading-lns approximation of  $T_{n \rightarrow m}$



Fig.14 : The leading-lms approximation for even signature amplitudes  $T_{2 \rightarrow 2}$ , as defined by its discontinuity

Fig.15 : The leading-lms approximation for the  $2 \rightarrow 3$  amplitude with signatures  $(\tau_1, \tau_2) = (-, +)$

Fig.16 : The leading-lms approximation for the  $2 \rightarrow 3$  amplitude with signatures  $(\tau_1, \tau_2) = (+, +)$

Fig.17 : Elements of the reggeon calculus for  $T^{(2)}$

Fig.18 : Reggeon diagrams for  $T_{2 \rightarrow 2}^{(3)}$  with odd signature

Fig.19 : Reggeon diagrams for  $T_{2 \rightarrow 3}^{(3)}$  with signature  $(-, -)$ .

Fig.20 : Lowest order perturbation theory for Figs.18 and 19

Fig.21 : Space time picture for the elastic photon-hadron scattering process in the Regge limit (rest frame of the photon)

Fig.22 : Elastic scattering of two  $q\bar{q}$ -systems in QCD: (a) the zero mass limit of  $T_{2 \rightarrow 2}^{(2)}$ ; (b) Parts of  $T_{2 \rightarrow 2}^{(4)}$  for which the zero mass limit can be shown to exist

Fig.23 : Elastic photon hadron scattering in QCD: on the lhs in the Bjorken limit, on the rhs in the Regge limit

Fig.24 : Space-time picture for the elastic photon-hadron scattering process in the Regge limit (CM-system): (a)  $T_{2 \rightarrow 2}^{(2)}$ ; (b)  $T_{2 \rightarrow 2}^{(4)}$

Fig.25 : (a) The total cross section as obtained in  $T_{2 \rightarrow 2}^{(2)}$ ; (b) the hadron extension in b-space for  $T_{2 \rightarrow 2}^{(2)}$  (massive case)

Fig.26 : Phase structure of reggeon field theory: the intercept of the renormalized Pomeron singularity is plotted against the bare negative mass. The two curves to the right of the critical point (dashed line) indicate the two solutions described in Refs. 41 and 42.

Fig.27 : Elements of supercritical RFT according to Ref. 42: (a) Pomeron creation and annihilation; (b) new diagrams which appear only in this phase of RFT; (c) interpretation of (b): new additions

to the triple -Pomeron vertex

Fig.28 : A part of the 2-2 reggeon vertex(a), as obtained in massive Yang-Mills theory, is identified as the "singular" vertex (b) of RFT (Fig.27c)

## References and Footnotes

- 1) For reviews of foundation and applications of perturbative QCD see, for example: J.Ellis, Lectures presented at the Les Houches Summer School 1976; H.D.Politzer, Physics Reports 14, 129 (1974)
- 2) For a discussion of this point I am grateful to Dr.J.Kwiecziński from Cracov, Poland.
- 3) A comprehensive review can be found in H.D.I. Abarbanel, J.B.Bronzan, R.L.Sugar, and A.R.White, Physics Reports 21c, 121 (1975)
- 4) M.Moshe, Physics Reports 37c, 257 (1978) and references therein
- 5) M.Gell-Mann and M.L.Goldberger, Phys.Rev.Letters 9, 275 (1962); M.Gell-Mann M.I.Goldberger, F.E.Low, and F.Zachariasen, Phys.Letters 4, 265 (1963); M.Gell-Mann, M.Goldberger, F.E.Low, E.Marx and F.Zachariasen, Phys.Rev. 133, B 145 (1964); M.Gell-Mann, M.L.Goldberger, F.E.Low, V.Singh, and F.Zachariasen, Phys.Rev. 133, B 949 (1964)
- 6) S.Mandelstam, Phys.Rev. 137, B 949 (1965)
- 7) H.Cheng and C.C.Lo, Phys.Lett. 57B, 177 (1975)
- 8) M.T.Grisaru, Phys.Rev. D 16, 1962 (1977); P.H. Dondi and H.R.Rubinstein, Phys.Rev. D 18, 4819 (1978)
- 9) K.Bardakci and M.B.Halpern, Phys.Rev. D6, 696 (1972)
- 10) L.F.Li, Phys.Rev. D9, 1723 (1974)
- 11) M.T.Grisaru, H.J.Schnitzer, and H.-S. Tsao, Phys.Ref. D8, 4498 (1973)
- 12) M.T.Grisaru, H.J.Schnitzer, and H.-S.Tsao, Phys.Rev. D9, 2864 (1974)
- 13) M.T.Grisaru and H.J.Schnitzer, Brandeis Preprint 1979
- 14) L.Lukaszuk and L.Szymanowski, Preprint of Institute for Nuclear Research, Warsaw, 1979
- 15) H.Georgi and S.L.Glashow, Phys.Rev.Lett. 32, 438 (1974)

- 16) M.C.Bergere and C.de Calan, Saclay preprint DPh -T/79-7
- 17) H.P.Stapp, in Les Houches Lectures 1975 (North-Holland, Amsterdam) p.159; A.R.White, *ibid.* p.427
- 18) V.N.Gribov, JETP 26, 414 (1968)
- 19) R.C.Brower, C.E.Detar and J.Weiss, Physics Reports 14c, 257 (1974)
- 20) J.Bartels, Phys.Rev. D11, 2977 and 2989 (1975)
- 21) J.Bartels, Nucl.Phys. B 151, 293 (1979)
- 22) I.N.Lipatov, Yadernaya Fiz. 23, 642 (1976)
- 23) E.A.Kuraev, L.N.Lipatov, V.S.Fadin, JETP 71, 840 (1976)
- 24) Ya.Ya. Balitsky, L.N.Lipatov, and V.S.Fadin in "Materials of the 14 th Winter School of Leningrad Institut of Nuclear Research 1979", p.109
- 25) E.A.Kuraev, L.N.Lipatov, and V.S.Fadin, JETP 72, 377 (1977)
- 26) J.Bartels, in preparation
- 27) V.N.Gribov in "Materials of the 8 th Winter School of Leningrad Institute of Nuclear Research 1973", p.5.
- 28) S.-J.Chang and S.-K. Ma, Phys.Rev. 188, 2385 (1969)
- 29) R.K.Ellis, H.Georgi, M.Machacek, H.D.Politzer, and G.G.Ross, CALT 68-684
- 30) H.T.Nieh and Y.P.Yao, Phys.Rev. D 13, 1082 (1976); B.M.McCoy and T.T.Wu, Phys.Rev. D 12, 2357 (1976) and Phys.Rev. D 13, 1076 (1976); L.Tyburski, Phys.Rev. D 13, 1107 (1976);
- 31) C.Y.Lo and H.Cheng, Phys.Rev. D 13, 1131 (1976) and Phys.Rev. D 15, 2959 (1977)
- 32) J.A.Dickinson, Phys.Rev. D 16, 1863 (1977)

33) H.Cheng, J.Dickinson, C.Y.Lo, K.Olausen and P.S.Yeung, Phys.Letters 76 B, 129 (1978)

34) H.Cheng, J.A.Dickinson, C.Y.Lo, and K.Olausen, Preprint 1977 and Stony Brook I TP-SB 79-7

35) P.Carruthers and F.Zachariassen, Physics Letters 62 B, 338 (1976)

36) J.B.Bronzan and R.L.Sugar, Phys.Rev. D 17, 585 (1978)

37) J.Bartels, unpublished

38) V.N.Gribov, L.N.Lipatov, and G.V.Frolov, Yad.Fiz 12, 994 (1971) Sov.Journ. of Nucl.Phys. 12, 543 (71)

39) H.Cheng and T.T.Wu, Phys.Rev. D1, 2775 (1970) and Phys.Lett.24, 1456 (1970)

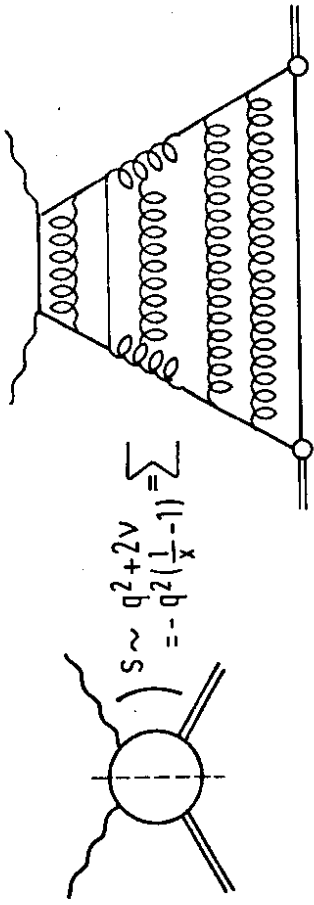
40) S.-J.Chang and P.M.Fishbane, Phys.Rev. D 2, 1104 (1970)

41) For a review of this solution see M.Le Bellac in "19 th International conference on High Energy Physics, Tokyo 1978", p.153 and references therein.

42) A.R.White, Ref.TH 2592-CERN

43) A.R.White, Ref.TH 2629-CERN

44) It should be emphasized that this argument is not strictly based on the reggeon calculus which has been derived in the previous section: there it was characterized as the  $g \rightarrow 0$  limit of the unitary S-matrix, and this approximation does not include renormalization of the parameters  $g, M^2$  etc. In order to use the concept of asymptotic freedom of  $g^2 (K_{\perp}^2)$  for large values of transverse momentum, as it is done in Ref.43, it is necessary to go beyond this approximation and include more nonleading terms. Whether this can be done in a consistent way, i.e. without destroying the subtle constraints of unitarity order by order in  $g^2$ , remains to be seen. It may also be that some of these new contributions are nonperturbative, i.e. they cannot be expanded in powers of  $g^2$  at all.



$$S \sim \sum_{\nu} q^2 + 2\nu = -q^2 \left( \frac{1}{\nu} - 1 \right) \sum$$

Fig.1

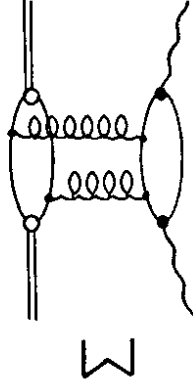


Fig.2

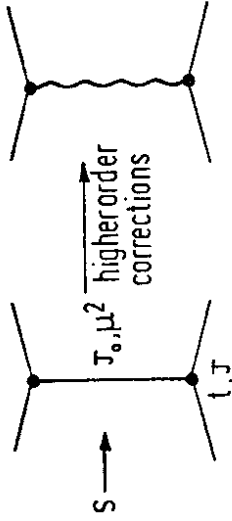


Fig.3

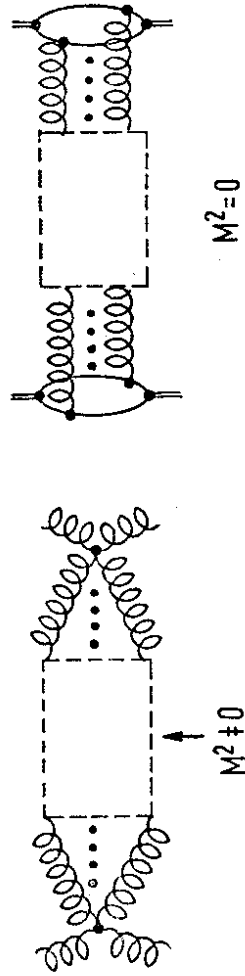


Fig.4

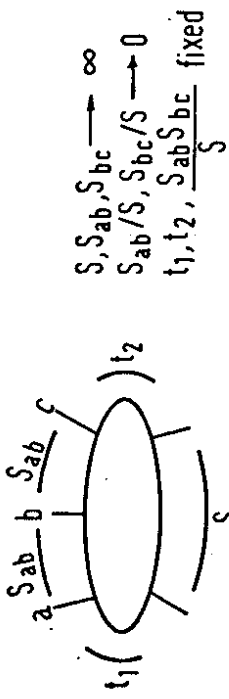


Fig.5

$$\begin{aligned}
 S, S_{ab}, S_{bc} &\rightarrow \infty \\
 S_{ab}/S, S_{bc}/S &\rightarrow 0 \\
 t_1, t_2, \frac{S_{ab} S_{bc}}{S} &\text{ fixed}
 \end{aligned}$$

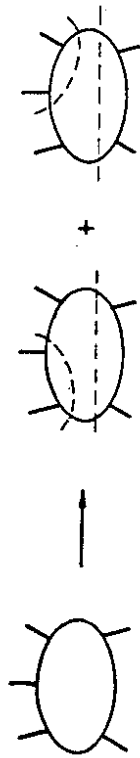


Fig.6

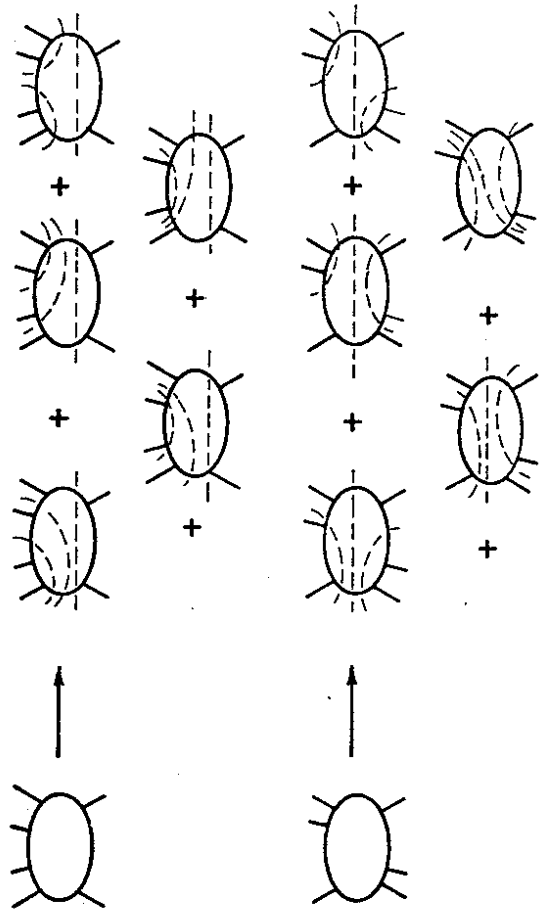


Fig.7

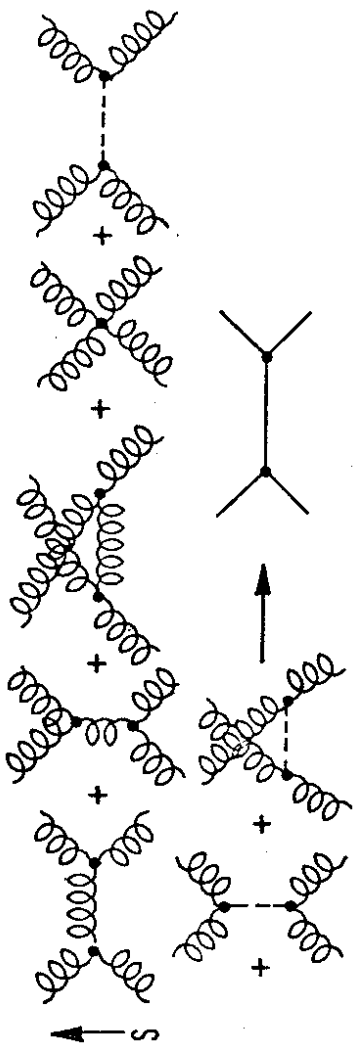


Fig.8

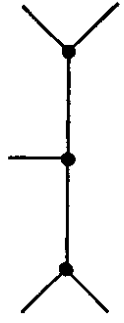


Fig.9

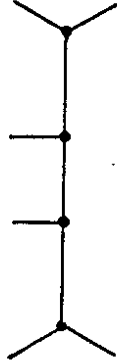


Fig.10



Fig.11

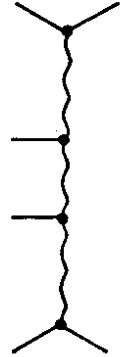


Fig.12

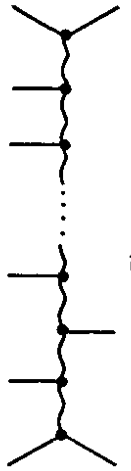


Fig.13

$$\text{disc } T_{2 \rightarrow 2}^{(2)} = \sum \left| \begin{array}{c} \text{even signature} \\ \text{even signature} \\ \text{even signature} \\ \dots \\ \text{even signature} \end{array} \right|$$

Fig.14

$$\text{disc}_{bc} T_{2 \rightarrow 3}^{(2)} = \sum \left| \begin{array}{c} \text{even signature} \\ \text{even signature} \\ \text{even signature} \\ \dots \\ \text{even signature} \end{array} \right|$$

Fig.15

$$\text{disc}_s T_{2 \rightarrow 3}^{(2)} = \sum \left| \begin{array}{c} \text{even signature} \\ \text{even signature} \\ \text{even signature} \\ \dots \\ \text{even signature} \end{array} \right|$$

Fig.16



Fig.17



Fig.18



Fig.19



Fig.20

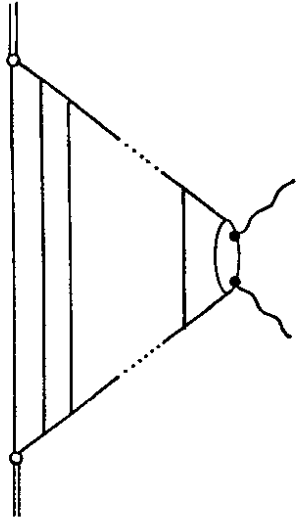


Fig.21

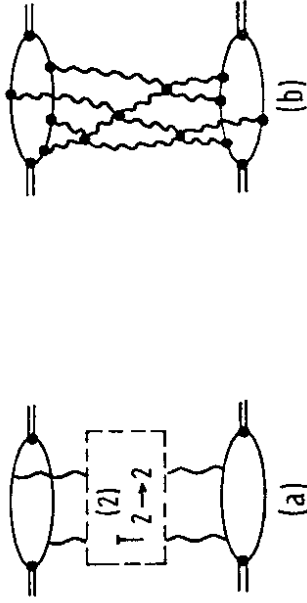
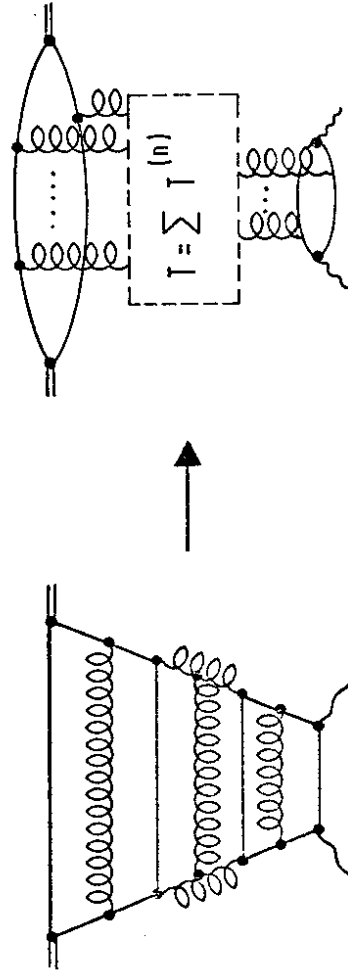


Fig.22



$q^2$  fixed,  $x \rightarrow 0$   
Regge limit

$X \neq 0, q^2 \rightarrow -\infty$   
Bjorken limit

Fig.23

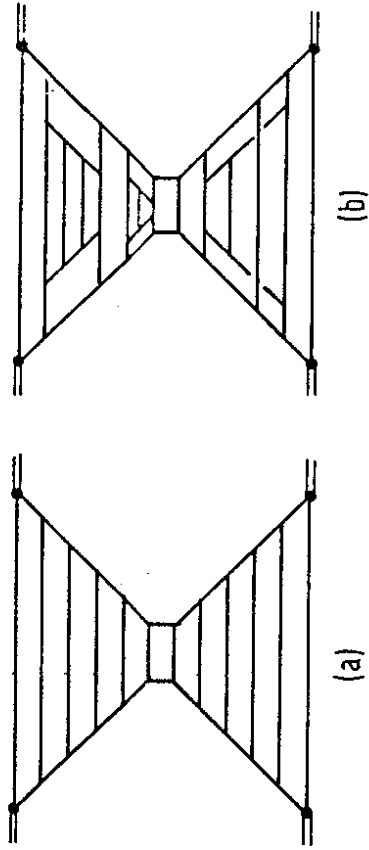


Fig. 24

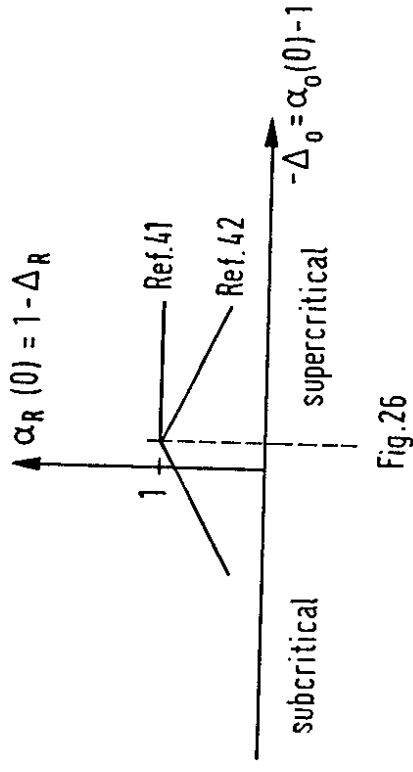
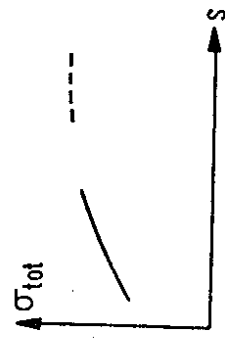


Fig. 25



a

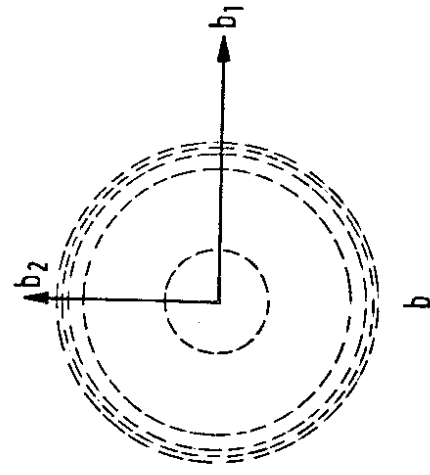


Fig. 25

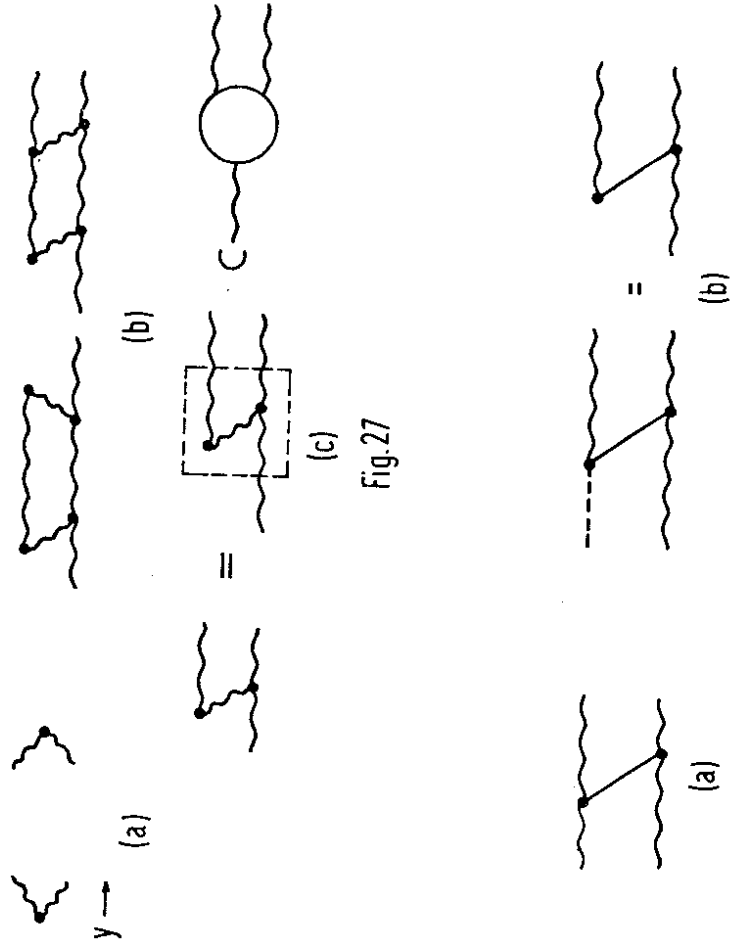


Fig. 27

Fig. 28